Geological Quarterly, 2025, 69, 71
DOI: https://doi.org/10.7306/gq.1844

Provenance and stratigraphy of the oldest sediments at the western slope of the East European Craton (Volyn-Orsha Rift, SE Poland) – constraints from detrital zircon geochronology

Jolanta PACZEŚNA[1, *], Paweł POPRAWA[2] and Ewa KRZEMIŃSKA[1]

[1] Polish Geological Institute – National Research Institute, Rakowiecka 4, 00-975 Warszawa, Poland; ORCID 0000-0003-2416-3907 [J.P.], 0000-0002-6832-8104 [E.K.]

[2] AGH University of Krakow, Faculty of Geology, Geophysics and Environmental Protection, al. Mickiewicza 30, 30-059 Kraków, Poland; ORCID: 0000-0002-9026-2252 [P.P.]

Pacześna, J., Poprawa, P., Krzemińska, E., 2025. Provenance and stratigraphy of the oldest sediments at the western slope of the East European Craton (Volyn-Orsha Rift, SE Poland) – constraints from detrital zircon geochronology. Geological Quarterly, **69**, 71; https://doi.org/10.7306/gq.1844

Associate Editor: Michał Zatoń

The Volyn-Orsha Rift (VOR) extends NE–SW, from the interior of the East European Craton (EEC) to its western margin. The basin is filled the oldest non-metamorphosed deposits in the craton, mainly with continental reddish to variegated sandstone of the Paliessie Group. It contains no stratigraphic indexes, therefore, its age remains ambiguous. Detrital zircon ages (SHRIMP) were investigated for sandstone from the lowermost part of the Polish Polesie formation in Kaplonosy IG 1 borehole to constrain the timing of its deposition and detritus provenance. Two dominant populations have been identified: yielding $^{207}Pb/^{206}Pb$ ages of ~1850–1750 Myr, interpreted as derived from denudation of the late Svecofennian proximal basement of the northern flank of the basin, and in a range of 1560–1450 Myr, typical of anorogenic within-plate granitoid batholiths, widespread in the Fennoscandia in the direct vicinity of the NW margin of the VOR. The remaining zircons (ages ~1290–1050 Myr) are interpreted as derived from the common Sveconorwegian-Grenville orogenic belt, in the Neoproterozoic riming the EEC from the west. The youngest six detrital zircons with $^{207}Pb/^{206}Pb$ age in the range of ~1082–1048 Myr, provide a new constraint on the possible deposition time. The true depositional age of this unit is probably younger (at least ~100 Myr) interpreted here as Neoproterozoic, due to an intracratonic position of VOR basin within the assembled Rodinia.

Key words: Volyn-Orsha Rift, Polesie formation, Neoproterozoic, detritus provenance, Pb-Pb dating on zircon.

INTRODUCTION

The oldest non-metamorphosed sedimentary cover of the western slope of the East European Craton is the Paliessie Group, composed of continental clastic red-beds and shallow marine deposits (Juskowiakowa, 1974; Makhnach et al., 1978, 2001; Wichrowska, 1992; Mikhnytska, 2013). This sediment is a fill of a large system of tectonic grabens of the Volyn-Orsha Rift (VOR), extending NE–SW, from the interior of the East European Craton (EEC) to the western margin of the EEC (Fig. 1; Bogdanova et al., 1996; Poprawa and Pacześna, 2002; Mikhnytska, 2013).

The stratigraphic age of this group is, therefore, of high significance for understanding the evolution of the sedimentary cover of the EEC, palaeogeography, and chronology of regional-scale tectonic processes. However, the Paliessie Group contains no index fossils, and its stratigraphic age remains ambiguous. It unconformably covers the metamorphic complexes and igneous belts adjacent to the suture of Fennoscandia and Sarmatia, generally not younger than 1.8 Gyr, being pierced by the anorthosite-mangerite-charnockite-granite (AMCG) suite at ~1.5 Ga (Fig. 2; Bibikova et al., 2009; Krzemińska et al., 2017).

In the Polish part of the VOR, the Paliessie Group is represented by an informal lithostratigraphic unit traditionally named the Polesie formation (Areń, 1974, 1982; Juskowiakowa, 1974) and is covered by the uppermost Ediacaran clastic and volcanic complex of the Żuków, Sławatycze and Teremiski Formations, from which it is divided by a large hiatus (Fig. 2; Pacześna, 2014). The U-Pb dating of zircons from tuffs within the Sławatycze Formation, being the component of the Volyn Large Igneous Province, allowed determination of its age as no older than ~580–570 Myr (Shumlyanskyy et al., 2016; Poprawa et al., 2020; Krzemińska et al., 2022).

* Corresponding author, e-mail: jpacz@pgi.gov.pl

Received: July 28, 2025; accepted: January 9, 2026; first published online: January 10, 2026

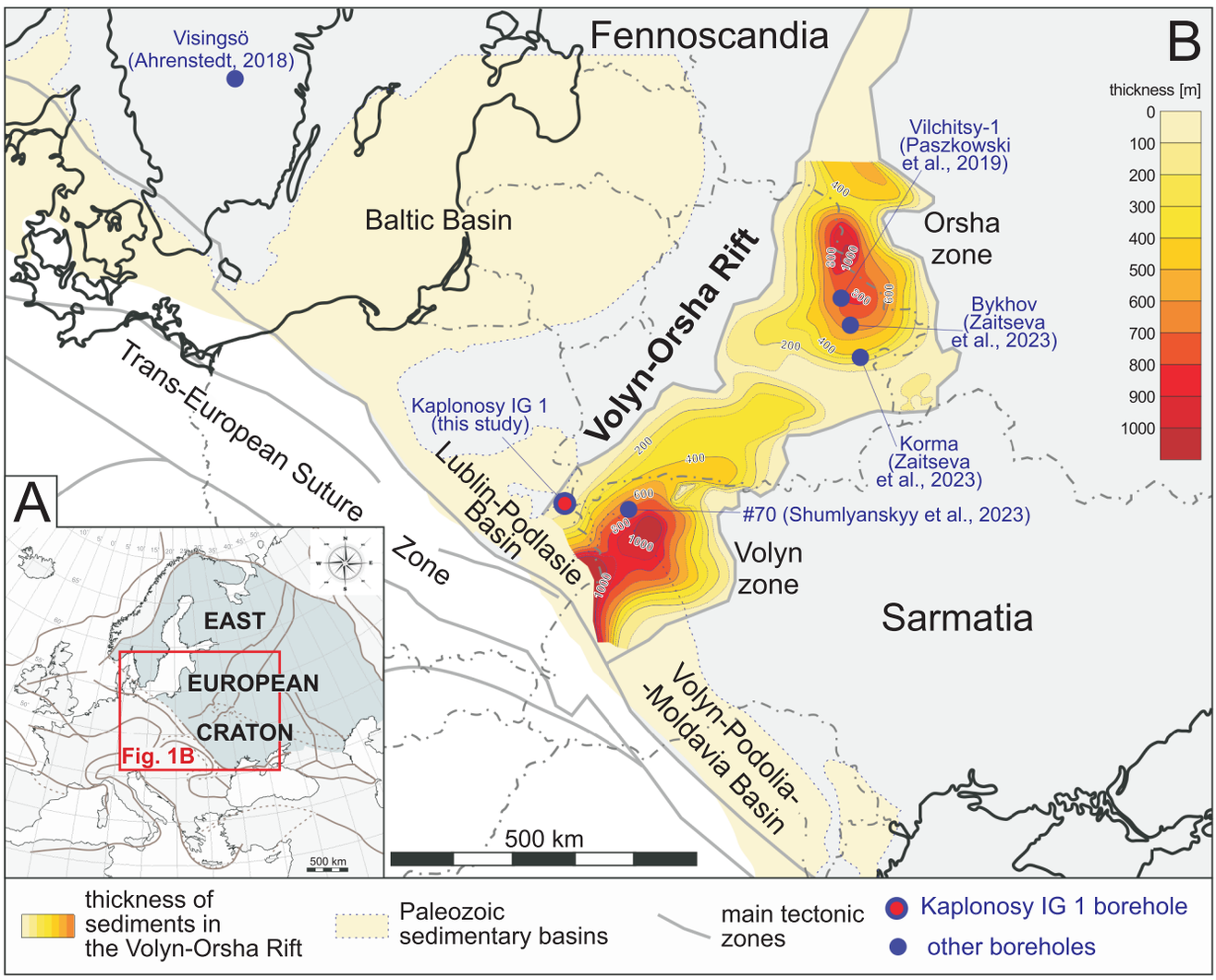

Fig. 1. Location of the Volyn-Orsha Rift and its relation to (A) the East European Craton (EEC) and (B) Lublin-Podlasie Basin (after Poprawa, 2019, 2020; Krzemińska et al., 2024), together with the location of the studied Kaplonosy IG 1 borehole (N51°37'13,42'', E23°21'24,47'')

B – the thickness map of the Polesie formation (Poland), in Belarus, including the Pinsk, Orsha, and Lapici formations, is compiled from the data of Gareckij et al. (1987) and Wichrowska (1992). The location of boreholes for which similar U-Pb dating on detrital zircon from the Polissia Group were conducted (Paszkowski et al., 2019; Shumlyanskyy et al., 2023; Zaitseva et al., 2023) and Neoproterozoic Visingsö Group of southern Sweden (Moczydłowska et al., 2017; Ahrenstedt, 2018) are also indicated

The above-mentioned data on the stratigraphy of the basement of the Polesie formation and the base of its overburden are highly unsatisfactory as constraints on the age of the formation's deposition, indicating that this process occurred over an extensive time span of nearly the entire Meso- and Neoproterozoic, i.e., nearly 1 Gyr. To narrow it down, we investigated Pb-Pb ages of detrital zircon for sandstone from two core samples, aiming to assess the maximum deposition age of the formation. This was supported by similar data from the Belarusian and Ukrainian parts of the VOR (Paszkowski et al., 2019; Shumlyanskyy et al., 2023; Zaitseva et al., 2023).

The other purpose of our U-Pb dating of detrital zircons from the Polesie formation sandstone is to determine detritus provenance. We regard it as key data for revealing the Proterozoic palaeogeography of the western EEC, detritus routing systems, and configuration of plates and orogenic belts in the direct vicinity of the EEC, thus, possibly having significance broader than regional.

GEOLOGICAL SETTING

REGIONAL PERSPECTIVE

The Volyn-Orsha basin is a Precambrian abandoned rift extending through the western and central EEC from the NW to SE (Fig. 1).

It is referred to as the Volyn-Orsha Rift (this study), the Volyn-Orsha Aulacogen (e.g., Bogdanowa et al., 2008), the Volyn-Orsha basin or depression (Shumlyanskyy et al., 2015, 2023), or the Volyn-Orsha Palaeotrough (Zaitseva et al., 2023). The sedimentary fill of its western part is composed mainly of continental reddish to variegated sandstone, mudstone, and nearshore claystone and mudstone of the Paliessie Group, the thickness of which reaches ~800–900 m in the depocentre in central part of the Volyn-Polesie Depression (Mikhnytska, 2013). It developed along the former suture of Fennoscandia and Sarmatia and Volgo-Uralia, being three once autonomous

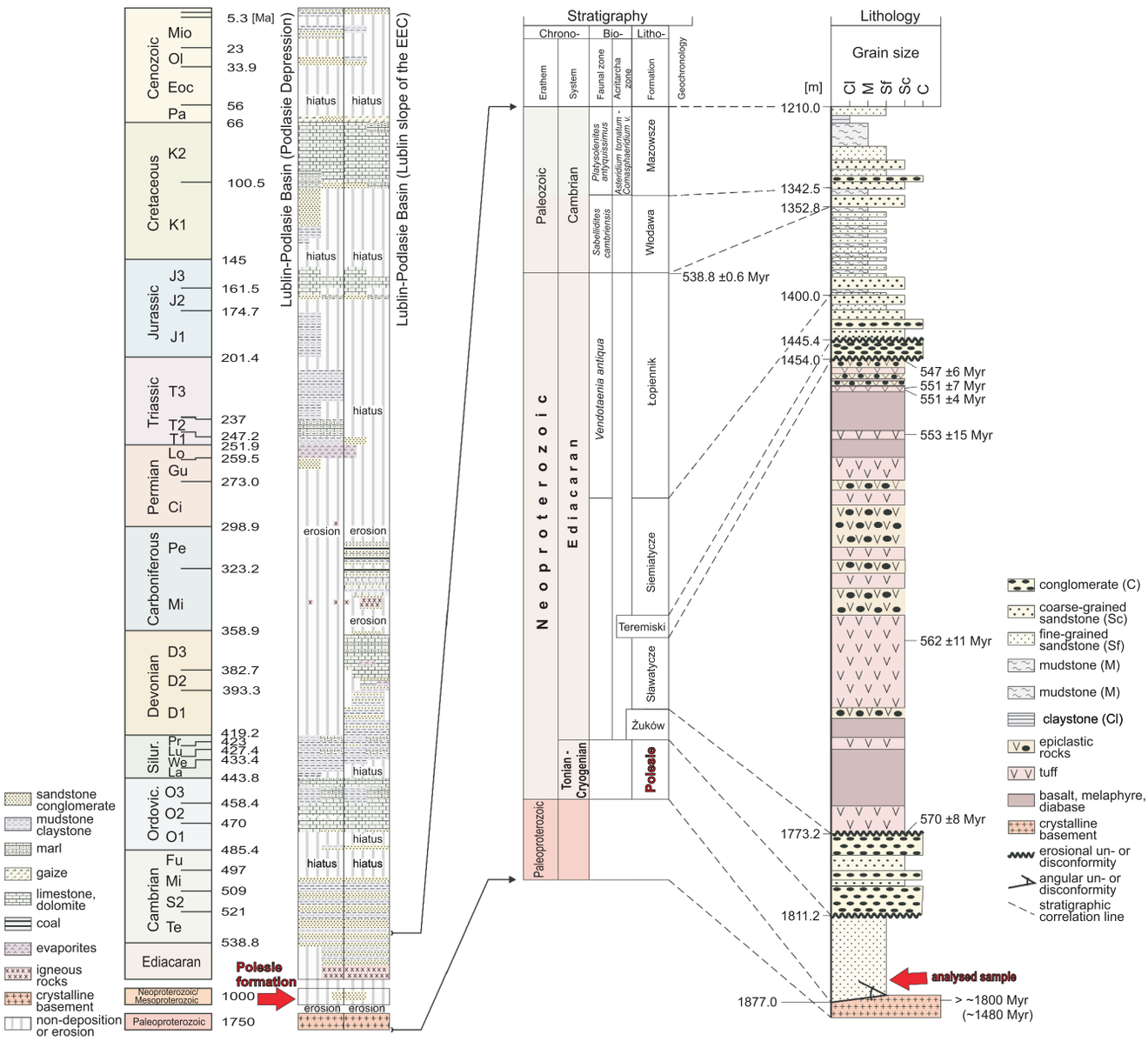

Fig. 2. Lithostratigraphic section of the Lublin-Lviv Basin with position of the Polesie formation (after Moczydłowska, 1991; Pacześna, 2010, 2014; Poprawa, 2019; Poprawa et al., 2020; Krzemińska et al., 2022; supplemented and modified)

Age of the overlying and underlying rocks gives broad constraints on the Polesie formation stratigraphic age

crustal segments together composing the EEC (Bogdanova et al., 1996, 2008). The crystalline basement of the western VOR is mainly the Osnitsk-Mikashevichi igneous belt (2.0–1.95 Ga), as well as the surrounding Okolovo terrane (2.0–1.9 Ga) and the Belarus-Podlasie granulite belt (1.9–1.85 Ga; Bibikova et al., 2009; Shumlyanskyy et al., 2015; Krzemińska et al., 2017).

In the western EEC, the VOR is buried beneath a succession of younger sedimentary basins, including the upper Ediacaran-lower Paleozoic, the Devonian-Carboniferous, and the Permian-Mesozoic ones (e.g., Modliński et al., 2010; Poprawa, 2019). Therefore, the deposits of Polesie formation is available for research only as core samples from the deep boreholes. Prior to the late Ediacaran, the VOR was a subject for long-lasting denudation, therefore, the youngest part of its sedimentary fill is not preserved.

The VOR is directly covered by the sedimentary succession of the Lublin-Podlasie Basin (Poprawa and Pacześna, 2002), part of an extensive system of the Ediacaran and/or lower Paleozoic basins of the SW slope of the EEC (Gareckij et al., 1987; Sliaupa et al., 2006; Poprawa et al., 2018; Poprawa, 2020). The development of the Lublin-Podlasie Basin was initiated with magmatic activity of the Volyn Large Igneous Province (Shumlyanskyy and Andréasson, 2004; Nosova et al., 2008; Środoń et al., 2019), interpreted as a synrift magmatism related to the break-up of the Rodinia/Pannotia supercontinent (Poprawa et al., 1999, 2020; Krzemińska et al., 2022).

Up-section, the Volyn flood basalts, agglomerates, and pyroclastics are replaced by continental to shallow marine clastic sediments of the uppermost Ediacaran to middle Cambrian (Fig. 2; Moczydłowska, 1991; Pacześna, 1996, 2006,

2010; Jaworowski, 1997), deposited during a transgressive to regressive cycle in the post-rift basin at the passive continental margin (Pacześna and Poprawa, 2005). The Lower and Middle Ordovician overlie the Cambrian with a hiatus and are composed of sandstone, shale, and limestone (Modliński, 1982; Modliński and Szymański, 2008). The Upper Ordovician and Silurian are represented by a facially monotonous complex of marine mudstone, claystone, and marl, partly bituminous, characterised by high thickness reaching several hundred metres (Fig. 2; Modliński and Szymański, 2008; Porębski and Podhalańska, 2019; Poprawa, 2020), deposited in the Caledonian foredeep basin related to the Avalonia-Baltica collision (Poprawa et al., 1999, 2018; Poprawa and Pacześna, 2002).

Age of the overlying and underlying rocks makes broad constraints on the Polesie formation stratigraphic age.

The Lower Devonian is a marine shelf, fine-grained, clastic sediment, passing up-section into alluvial clastic deposits, while the Middle and Upper Devonian are dominated by carbonates, locally with evaporite and clastic interbeds (Fig. 2; Miłaczewski and Radlicz, 1974; Miłaczewski, 1981; Narkiewicz et al., 1998). During the Mississippian time, the development of the basin was interrupted by tectonic deformation, uplift, and denudation, terminated with intensive alkaline magmatism covering the area between the Lublin and Baltic regions (Poprawa et al., 2024; Krzemińska et al., 2025). The subsequent Carboniferous basin accumulated shallow shelf, deltaic, and fluvial sediments (Waksmundzka, 1998), in the lower part mostly carbonate and fine-grained clastics, while in the upper part mostly sandstone and mudstone, with a characteristic contribution of hard coal (Fig. 2; Żelichowski, 1972; Porzycki and Zdanowski, 1995).

Following the late Variscan tectonic deformation, uplift, and denudation, an early Permian episode of magmatic activity took place in the study area (Krzemińska et al., 2021). In the Late Permian and throughout the Mesozoic, this area became the eastern flank of the Polish Basin, characterised by the presence of common hiatuses, covering a significant part of late Permian and Mesozoic time span (Dadlez and Marek, 1997). The Cenozoic is an unconsolidated, clastic sedimentary cover of low thickness (Piwocki and Kramarska, 2004).

THE POLESIE FORMATION

The oldest, unmetamorphosed sediments were deposited on eroded Paleoproterozoic crystalline basement rocks as the siliciclastic Polesie formation (Areń, 1982; Juskowiakowa, 1974). They were accumulated mainly within a narrow, NE-SW elongated tectonic graben, thus they were recognized locally in SE Poland, e.g. in the Kaplonosy IG 1, at depths ranging from 1811 m to 1877 m and Busówno IG 1 boreholes, from a depth of 4082.0 m to the borehole end at 4154.5 m (Fig. 3A, B). The sedimentary rocks rest on a thin zone of weathered rock, the nature of which indicates mechanical weathering and basement disintegration, with the formation of a small layer of weathered clays. In Busówno IG 1, it is a red-coloured, fine-grained, quartz sandstone, with interbeds of fine-grained grey sandstone. Although macroscopically rather monotonous (Fig. 4A, B), they sometimes contain thin clay layers. They are considered to be epicontinental or continental and marginal-marine deposits (Wichrowska, 1992; Pacześna, 2007) dominated by quartz arenites with minor constituents of mud and coarser sediments. These rocks are characterized by a weak to sub-angular rounding of grains and a variable degree of sorting. They are composed mainly of sand-sized (0.0625 to 2 mm) silicate grains (quartz: 50 to 60%), accompanied by alkali feldspar (orthoclase and microcline) and plagioclase feldspar (albite). Mica grains occur as random tiny fragments or elongated flakes (ranging between 1–3%). The heavy minerals, like zircon, rutile, and/or tourmaline, occur only in traces (Fig. 4A, B), but their concentration increases towards the top. The sandstones of the Polesie formation are cemented with silica, carbonate, or hematite.

The Polesie formation is the westernmost part of a significant lithological complex the Paliessie Group which has broad regional lithostratigraphical significance in the VOR. In the chronostratigraphical framework this lithostratigraphical unit is an equivalent of the Paliessie regional stage or horizon (Makhnach et al., 2001; Zaitseva et al., 2023). Deposits of Paliessie Group filled of most tectonic grabens of the VOR. The thickness of Paliessie Group reaches 170 m in northern Byelarus in the Orsha sub-basin of VOR (Makhnach et al., 2001) and maximum 900 m in the Volyn-Polesie sub-basin of VOR in a centre of the Volyn-Polesie Depression in the Ukraine (Mikhnytska, 2013). At the most area of the VOR the Paliessie Group covers crystalline rocks of lower Proterozoic basement of EEC represented by 1.2 Gyr gneisses and granitoids and 1–1.1 Gyr gabbro intrusions (Makhnach et al., 2001; Mikhnytska, 2013). Locally, in the Orsha Depression it lies on the deposits of older Sherovici Group. The sedimentary cover of Paliessie Group is composed of red-beds mainly of fine-, rarely coarse-grained sandstone with hematite intercalated with grey to brown siltstone or clay and thin beds of conglomerate. Sediments of Paliessie Group originated in the broad spectrum of sedimentary environments mainly in the very shallow epicontinental basins with reduced salinity. Part of these sediments were deposited on the wide alluvial plain with deposition in the braided river channels and streams periodically flooded by a short duration marine ingression (Makhnach et al., 2001).

ANALYTICAL METHODS

ZIRCON SEPARATION AND SAMPLE PREPARATION

In the sandstone collected from the lowermost part of the Polesie formation, depth of 1875.0 m, a change in the colour of the sediment was observed from dominant red to grey (Fig. 3A). For this reason, this fragment of the drill core was cut into two separate pieces (Fig. 4B, C). The zircon separation procedure for each of them was carried out separately. This resulted in two individual samples designated as Kap-1875j, a grey part, and Kap-1875c, a reddish part.

For the separation of detrital zircons, the cut pieces of the drill core were crushed using a jaw crusher. The samples were further pulverized using a ring mill and then filtered through a few sieves up to 63 μm. Heavy minerals were obtained from the particles separated using water panning and heavy liquids. The magnetic minerals were removed using a hand magnet. The remainder underwent a series of magnetic separations by Frantz barrier separator. All detrital zircons were individually isolated manually using a binocular microscope. An epoxy resin megamount of 35 mm diameter disc for U-Pb analysis was prepared together with the separated detrital zircons and the reference zircon grains.

The grain-rows of each sample were photographed in transmitted light and reflected light using the optical *NIKON* microscope with *ECLIPSE LV100POL* system. To identify the internal structures of the detrital zircons, back-scattered electron (BSE) and cathodoluminescence (CL) images were obtained using a scanning electron microscope (*Hitachi Su 3500*) installed at the Polish Geological Institute – National Research Institute. Analytical points were mainly selected as rims of detrital zircons, while fractures, mineral inclusions, inherited cores, and metamorphic overgrowth parts were eliminated after the CL and BSE image observation.

Fig. 3. The drill core samples showing a typical feature of arcosic sandstones from the Polesie formation

A – large-scale cross-bedded fine-grained sandstone with very thin coarse- grained sandstone intercalations, Busówno IG 1 borehole, depth 4146. 4 m; **B** – Kaplonosy IG 1 borehole, depth 1875.5 m (the bottom part of the formation) collected for detrital zircon age study (divided into two sub-samples; **C** – sample Kap-1875.5 j; **D** – sample Kap-1875.5c

U-Pb ANALYSIS

All detrital zircon U-Pb age determinations were performed using a Sensitive High-Resolution Ion Microprobe (SHRIMP IIe/MC) at PGI-NRI. The diameter and current of the O_2^- primary ion beam were ~20–23 μm and 3.0–4.0 nA, respectively. The reference zircon 91500 was used for quantitative calibration of U concentration (78 ppm; Wiedenbeck et al., 1995; Williams, 1998). U-Th-Pb ratios were determined relative to the TEMORA2 (416.8 Myr, $^{206}Pb^*/^{238}U = 0.06683$) reference zircon (Black et al., 2003) analyzed repeatedly during the analytical session. Data acquisition for zircon during each session involves analysis of the TEMORA2 reference zircon, performed after every three sample analyses. A Supplementary Table 1 contains the full analytical dataset from SHRIMP comprising analyses of the reference TEMORA 2 grains.

Details of the analytical procedures can be found in Williams (1998). The SHRIMP data reduction was handled using *SQUID 2.5* (Ludwig, 2009). All uncertainties are quoted at the one-sigma level. To construct the concordia curve and determine the concordia age, as well as probability plots showing an age distribution, the *Isoplot 3.71* (Ludwig, 2008) was applied.

Individual corrected ratios and dates are reported with 1 precision estimates. U-Pb concordia ages and weighted mean age diagrams were calculated using the program *Isoplot/Ex 3.0* of Ludwig (2003). Age calculations are based on IUGS recommended values for U decay constants (Steiger and Jäger, 1977). The statistical coherence of calculated means is assessed using the mean square of weighted deviation (MSWD; McIntyre et al., 1966).

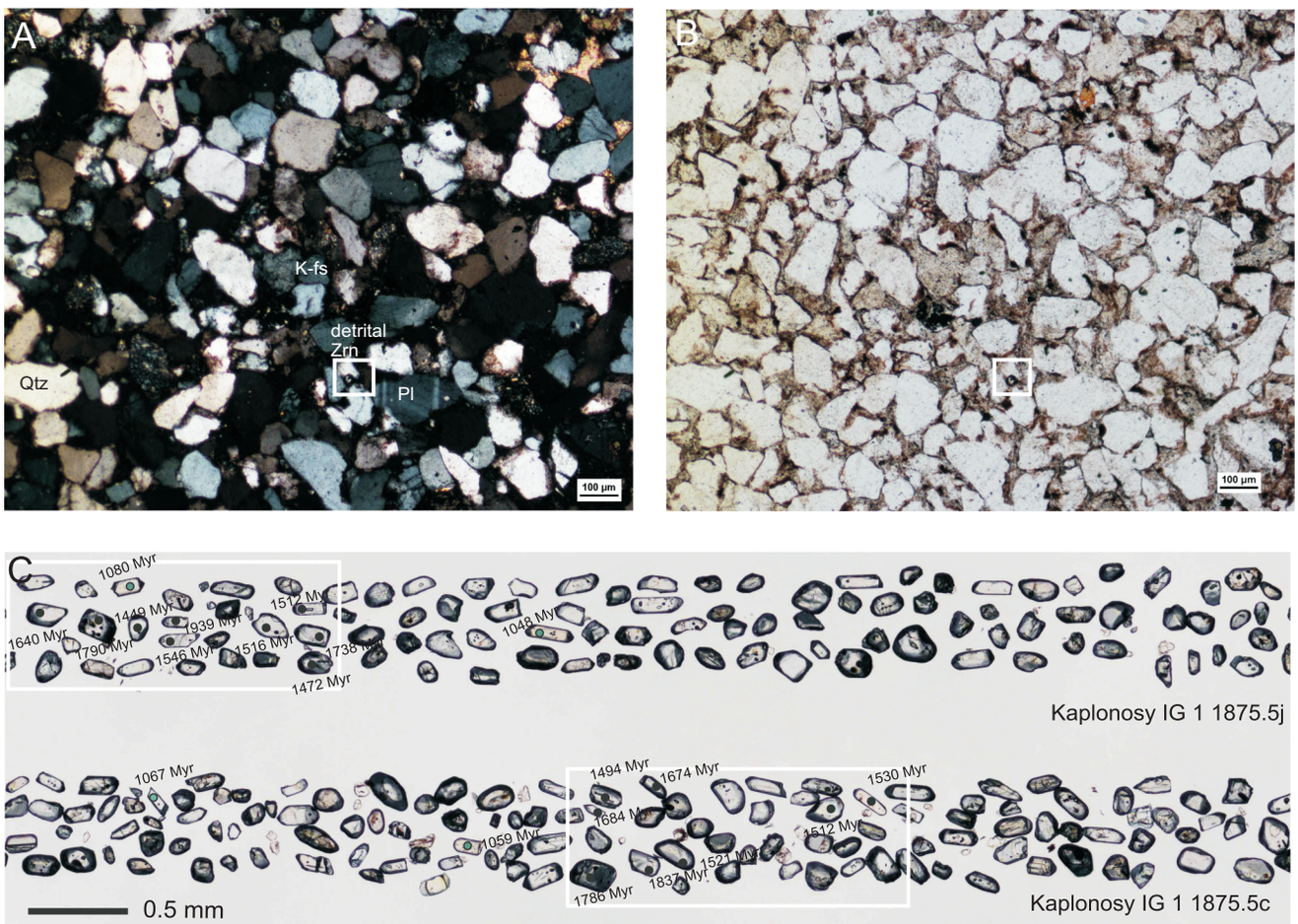

Fig. 4. Photomicrographs of the sandstone sample (thin-section view of the same microarea) from the lower part of Polesie formation (Kaplonosy IG 1 borehole) showing

A, **B** – a mineral assemblage with sub-rounded grains dominated by quartz, feldspars, and zircons as an accessory phase including zircon, indicated by a white frame; **C** – transmitted light image of zircon grains morphology from both subsamples, with locations of some SHRIMP analyses. The position of the representative CL zircon images presented in Figure 5 is marked with the white frame. Photographs were taken: (A) under crossed polars, (B, C) plane polars, transmitted light, including the image of detrital zircon grains (Kap-1875.5j and Kap-1875c) selected for age study. Scale bar is 100 µm for A, B and 500 µm for C

Following common practice, the SIMS $^{207}Pb/^{206}Pb$ ages were used directly for zircons older than 1 Gyr, but $^{206}Pb/^{238}U$ ages for those younger, although the exact cut-off values vary considerably in the literature (e.g., 1.2 Gyr; Spencer et al., 2016). In this case, the choice was more aligned with earlier publications that were used for correlation.

The final detrital zircon data processing encompassed an evaluating the difference between samples using objective methods, a non-parametric statistic test to recognize a dissimilarities of the matrix, including Multi-Dimensional Scaling (MDS) map for zircon populations calculated using both Wasserstein and Kolmogorov-Smirnov distance. The results were visualised on the MDS plots (Vermeesch, 2012, 2013), generaded using *Isoplot R* toolkit (Vermeesch, 2018).

RESULTS

SHRIMP DETRITAL ZIRCON AGES AND POPULATIONS

The analyzed detrital zircon crystal morphologies ranged from euhedral to anhedral. Both samples (Kap-1875j and Kap-1875c) of the Polesie formation are characterized by a diversity of detrital grain forms, including rounded and angular (Fig. 4C), with colours ranging from almost clear to reddish or light brownish. The size of the grains ranged between ~40–150 µm, As a detrital cargo of this sample, a less rounded grains, and those that have rougher surfaces were also identified. There are no significant differences between the grain collections from both subsamples. Cathodoluminescence (CL) images of representative detrital zircon grains (Fig. 5) disclose, that a most grains have clear oscillatory zoning that is indicative of a magmatic origin, whereas others have weak or banded oscillatory zoning of mafic magmatic or metamorphic origin. The CL images of individual detrital zircons from the youngest populations of mostly prismatic crystals are shown separately (Fig. 5C) to demonstrate their various (mostly simple) oscillatory zoning and no inherited material.

A total of 84 and 82 analysis points were measured in zircons from each sample for the U-Pb ages. The U-Pb age data for the detrital zircon grains are given in supplementary material (Supplementary Table 1). Most analyses were concordant or nearly concordant (Fig. 6A, C), within analytical uncertainty. The few exceptions showed evidence of significant loss of radiogenic (Supplementary Table 1). Consistent with their common detrital origin, the analysed zircons had a wide range of U-Pb isotopic compositions, with the most concordant $^{207}Pb/^{206}Pb$ ages ranged from 1972 Myr to 1080 Myr (Kap-1875j) and from 1987 Myr to

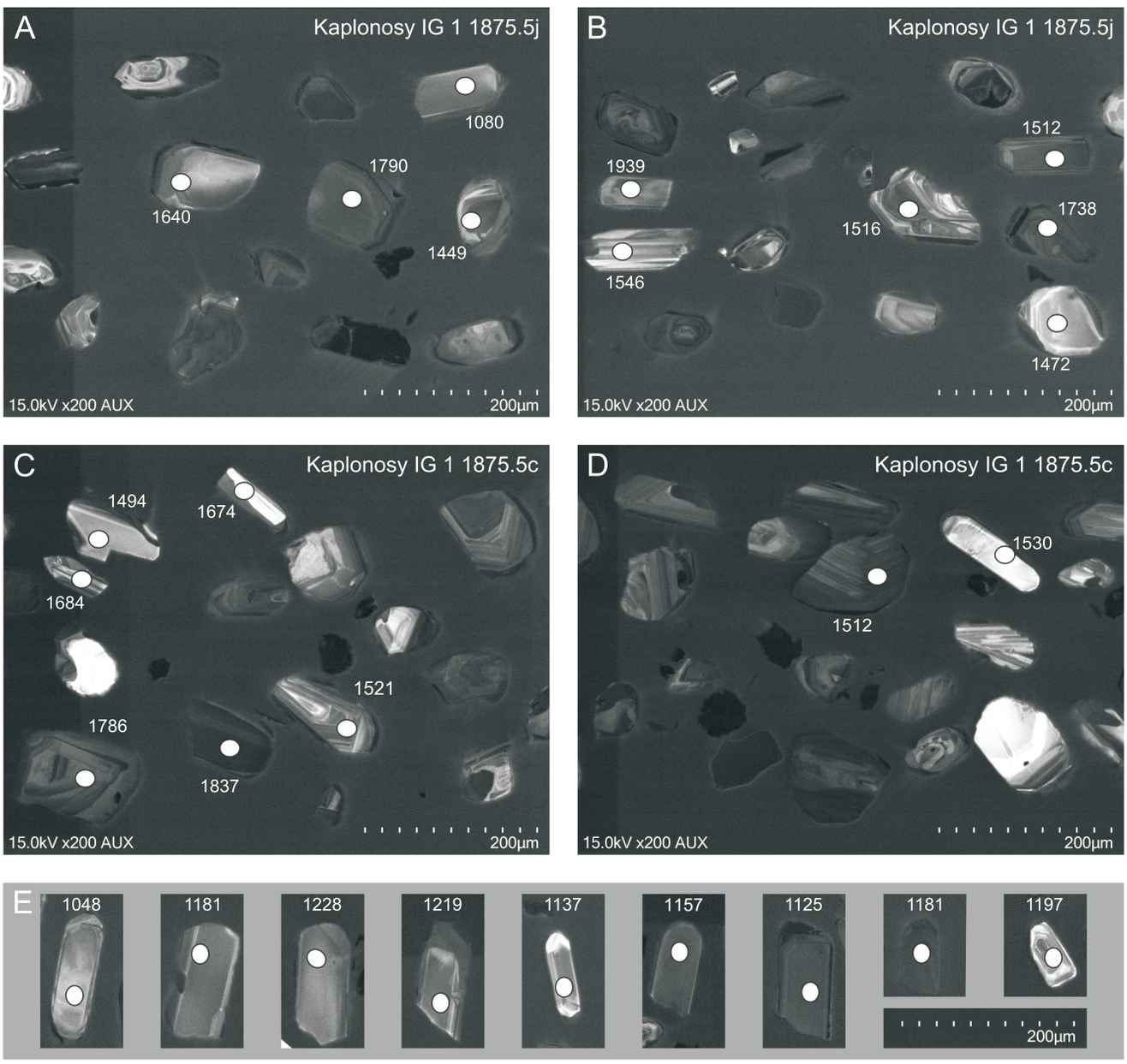

Fig. 5. The characteristics of representative detrital zircon grains disclosed by cathodoluminescence imaging CL accompanied with selected images of single zircons representing a relatively youngest age group

The morphology of some grains is visible in the transmitted light photos. SHRIMP analyses are located and labelled with their $^{207}Pb/^{206}Pb$ ages (in Myr)

1067 Myr (Kap-1875c; Fig. 6A, C). The detrital zircons is dominated by two clusters (Fig. 6B, D) of the Orosirian age, with peaks on a density probability plot at 1807 or 1802 Myr, and the Calymmian age, with peaks at 1515 or 1514 Myr. There is also a minor group of the Stenian grains. There is no Archean or early Paleoproterozoic (i.e. Siderian and Rhyacian) detritus. Apart from the youngest group, the age distribution of the population seems to be bimodal. The age peaks seem to be analogous. This small diversity led to the use of the Unimix age isoplot tool to better define the peaks and clusters. This shows that both parts of the sandstone that differ in colour contain almost identical detrital zircon groups (Table 1).

To constrain the maximum depositional age of the Paliessie Group, which was one of the main purposes of this study, the analysis was preferentially performed on transparent euhedral detrital zircon grains with simple oscillatory zoning that are thought to have the youngest age and origin. The age of the youngest detrital zircons for both samples (Supplementary Table 1) ranges between ~1080 (+0%disc)–1048 (–16%disc.) Myr (two grains) and 1082 (–6%disc) –1059 (–3%disc) Myr (four grains). Thus, each sample shows relatively similar ages of the youngest cluster (Table 1). Due to this similarity and the uneven content of the few youngest zircons, for the calculation of the concordia age (c.a.) and the weighted average (w.a.) data for both samples were combined. A merged data are showed on the Wetherill cand Tera-Wasserburg condordia plots (Figs. 7F, 8D).

Apart of the $^{207}Pb/^{206}Pb$ detrital zircon age spectra (Fig. 7), Th/U values of analysed grains were used to discriminate between metamorphic origin (Th/U < 0.1) and magmatic origin (Th/U > 0.1), for this purpose all analysed zircons were used

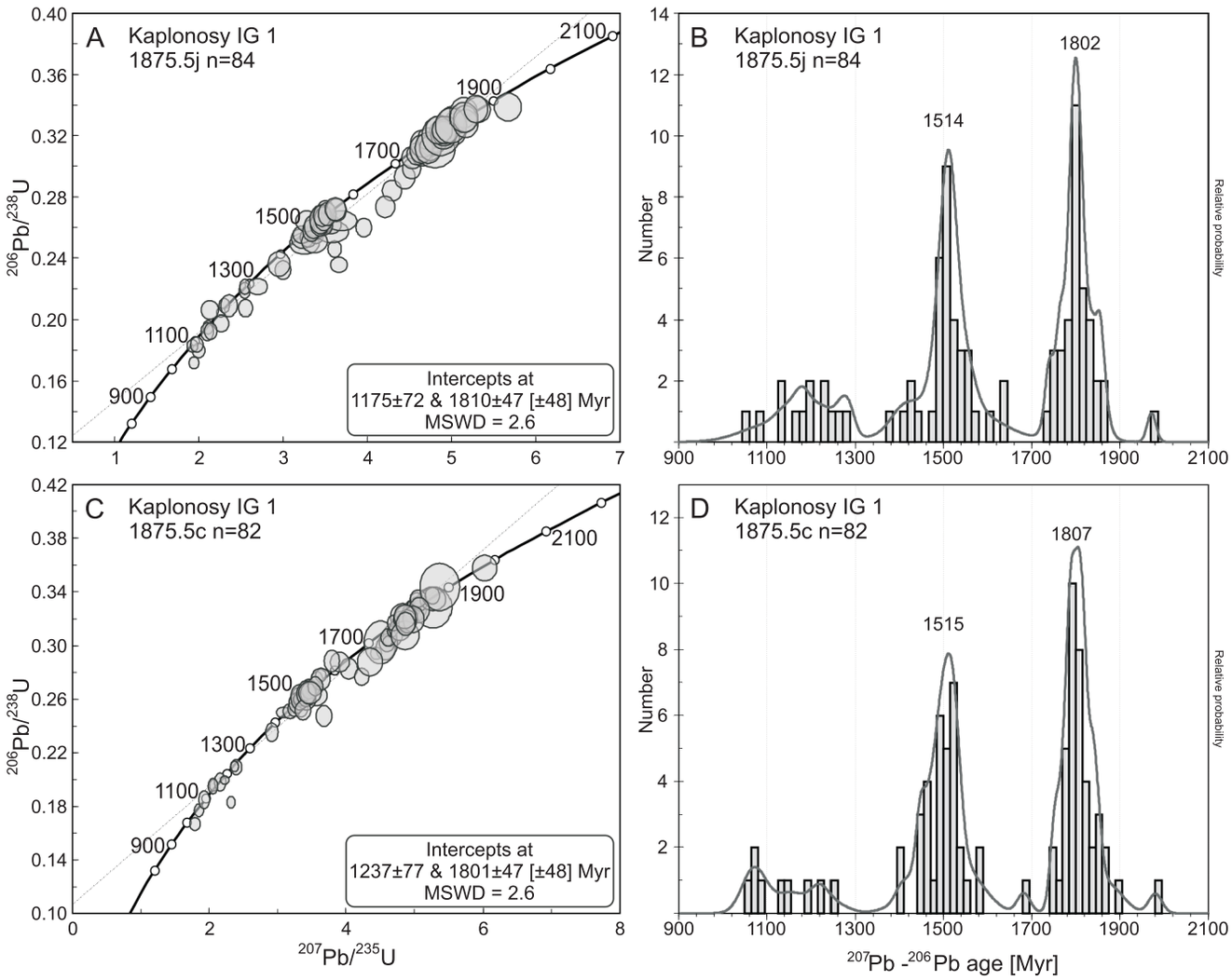

Fig. 6. Results of the SHRIMP U-Pb dating of detrital zircons of the Polesie formation Kap-1875.5 Concordia diagrams and Probability density plot (PDP) diagrams, displaying ages from the main zircon populations in the analyzed sub-samples

(Supplementary Table 1). The grains with Th/U < 0.1 , typical of metamorphic crystallisation, are rare within all compared samples (Fig. 9).

DISCUSSION

CHARACTERIZING A POTENTIAL PROVENANCE AREAS

The provenance of sedimentary material can be assessed by comparing its detrital zircon ages with geochronological characteristics of the potential source areas. The detrital zircons from the lowermost part of the Polesie formation can be split by age peaks into three major groups, including the late Paleoproterozoic (Orosirian) group with the age peaks at 1807 and 1802 Myr, the early Mesoproterozoic (Calymmian) group, with the age peaks at 1515 and 1514 Myr), and the Mesoproterozoic (Stenian) group with relatively smaller number of grains, indicating that both late Paleoproterozoic and Mesoproterozoic magmatic activity was intense in the provenance region. The crystalline basement with that age pattern extends over a vast area of central Fennoscandia from the southern Baltic offshore (Amberland Domain) to the edge of the EEC (Bogdanova et al., 2006, 2015; Krzemińska et al., 2017;

Table 1

The summary of the U-Pb detrital zircon age results obtained for the lowermost part of Polesie formation in Kaplonosy IG 1 borehole, depth 1875.5 m

Sample ID	n=	Range [Myr]	Group I [%]	Group II [%]	Group III [%]	Pb-Pb age [Myr] youngest grains (YSG)
Kap-1875j	84	1080 1972	1811.8 ±4 [43%]	1511.6 ±7 [41%]	1144.3 ±11 [15%]	1080, 1048
Kap-1875c	81	1067 1981	1800.9 ±4 [49%]	1487.6 ±7 [40%]	1103.3 ±17 [11%]	1067, 1082, 1059, 1078
Kap-1875.5 merged	166	1067 1981	1807 ±1.4 [46%]	1500.5 ±2.4 [41%]	1133 ±4.5 [13%]	1067 ±16 (c.a) 1071 ±11 (w.a)

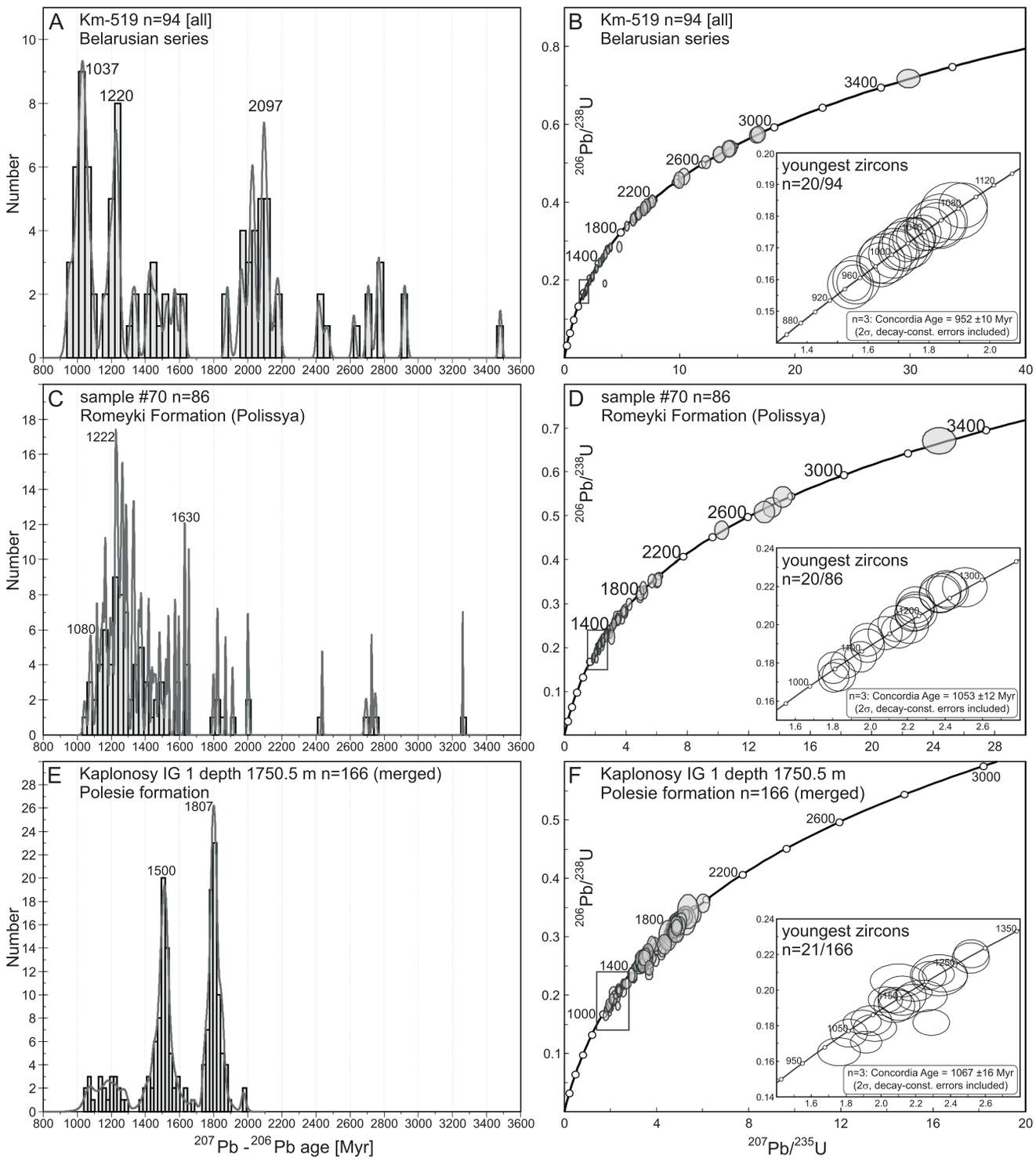

Fig. 7. The Polesie formation detrital zircons characteristics compared with the data for its lateral equivalents

A, **B** – sample Korma-519 Rudnya Formation in Belarus (after Zaitseva et al., 2023); **C**, **D** – sample #70, Romeyki Formation in Ukraine (after Shumlyanskyy et al., 2023); **E**, **F** – sample Kap-1875.5 merged (this study)

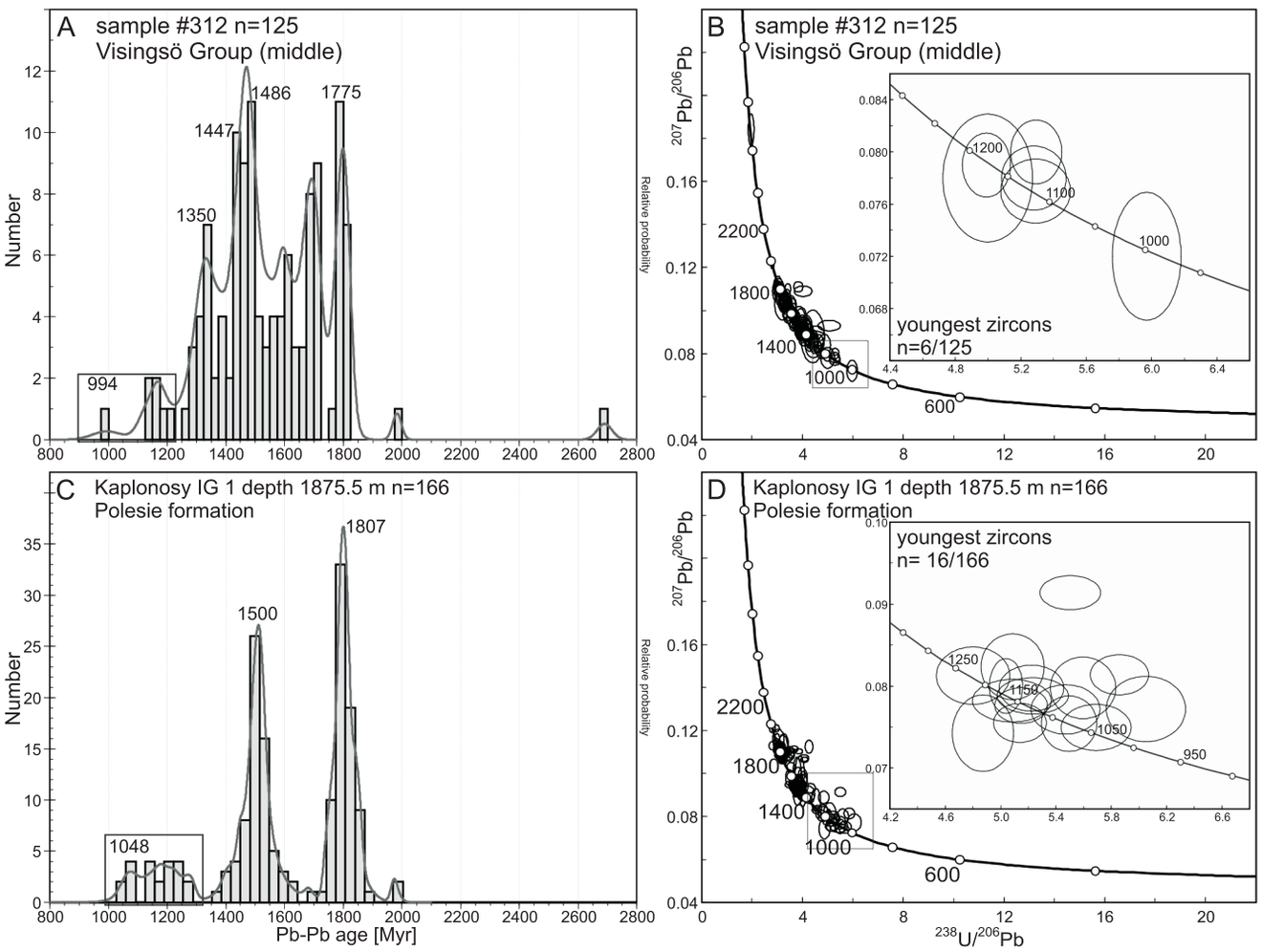

Fig. 8. The Polesie formation detrital zircons characteristics compared to Late to post-Sveconorwegian sediments of the Visingsö Group, southern Sweden sample #312 (after Ahrenstendt, 2018)

Skridlaite et al., 2021). This age range is typical of the syn- to late-orogenic intrusions in the Svecofennian orogen, that constitute most of the south-western Fennoscandia (Bodganova et al., 2015; Skridlaite et al., 2021; Krzemińska et al., 2021). The centre of Fennoscandia hosted an episodic Mesoproterozoic (~1.53–1.50 Gyr) continental magmatism of the anortnosite-mangerite-charnockite and granite (AMCG) suites extending from central Sweden and Finland to Poland (e.g., Bingen et al., 2008; Wiszniewska and Krzemińska, 2021). All emplaced between the 1.55–1.53 Ga (Salmi suite), 1.65–1.61 Ga (Wiborg suite), 1.59–1.56 Ga (Åland suite), and 1.53–1.50 Ga (Mazury Complex). reflect an intracontinental extensional setting. The age pattern with two major age peaks well corresponds to the time of formation of the crystalline basement located directly to the north of the Kaplonosy IG 1 borehole. A relatively proximal source type are would also be indicated by the presence of the significant number of poorly rounded zircons and other detrital components (Fig. 4). Despite a fine-grained fraction of the sediment, no particularly exotic material from distant sources has been identified here. The characteristics of detrital material obtained from sample Kap-1875.5 almost unequivocally indicate dominance of a local type of source (i.e. > 85% grains), represented by ~1.8 Gyr and ~1.5 Gyr zircons (Fig. 6), that must have come from the eroded topographic highs, exposing the late Svecofennian (1.85–1.74 Ga) basement of the EEC intruded by the AMCG (1.53–1.48 Ga) massifs (Krzemińska et al., 2017; Wiszniewska and Krzemińska, 2021; Grabarczyk et al., 2023). The very similar detrital zircon cargos were also noted in younger layers, e.g. Ediacaran, in clastic rocks, including pyroclastic rocks accompanying the Sławatycze Formation (Poprawa et al., 2020). The peaks at 1.5 Gyr and 1.8 Gyr in detritus have for a long time constituted a legible signature of the basement at the SW margin of EEC (Żelaźniewicz et al., 2020).

Similarly a local source has been concluded for quartz rich sediments of the Orsha sub-basin (Zaitseva et al., 2023; Shumlyanskyy et al., 2023), on the basis detrital zircon age pattern, and for sedimentary fill of the Volyn sub-basin where a relatively poorly-sorted, poorly-rounded, subarcosic detritus was recognized.

A simple comparison of the detrital zircon age distribution (Fig. 7A–F) between VOR sediments revealed a significant differences of the age patterns, which can be explained by a differences in the age of the eroded local basement i.e. a specific crustal units within the EEC. A common feature of the detrital fill remains however a deposition of the material younger than 1.2 Gyr. All of the sediments from VOR listed in the diagrams are characterized by the presence of late Mesoproterozoic zircons.

This also applies to the results of the Kap-1875.5 (Fig. 7E) sample, where almost bimodal detrital age pattern is accompanied, with the third, lesser group represented by n=12/166 (12.6%) grains yielding $^{207}Pb/^{206}Pb$ ages of ~1.29–1.05 Gyr

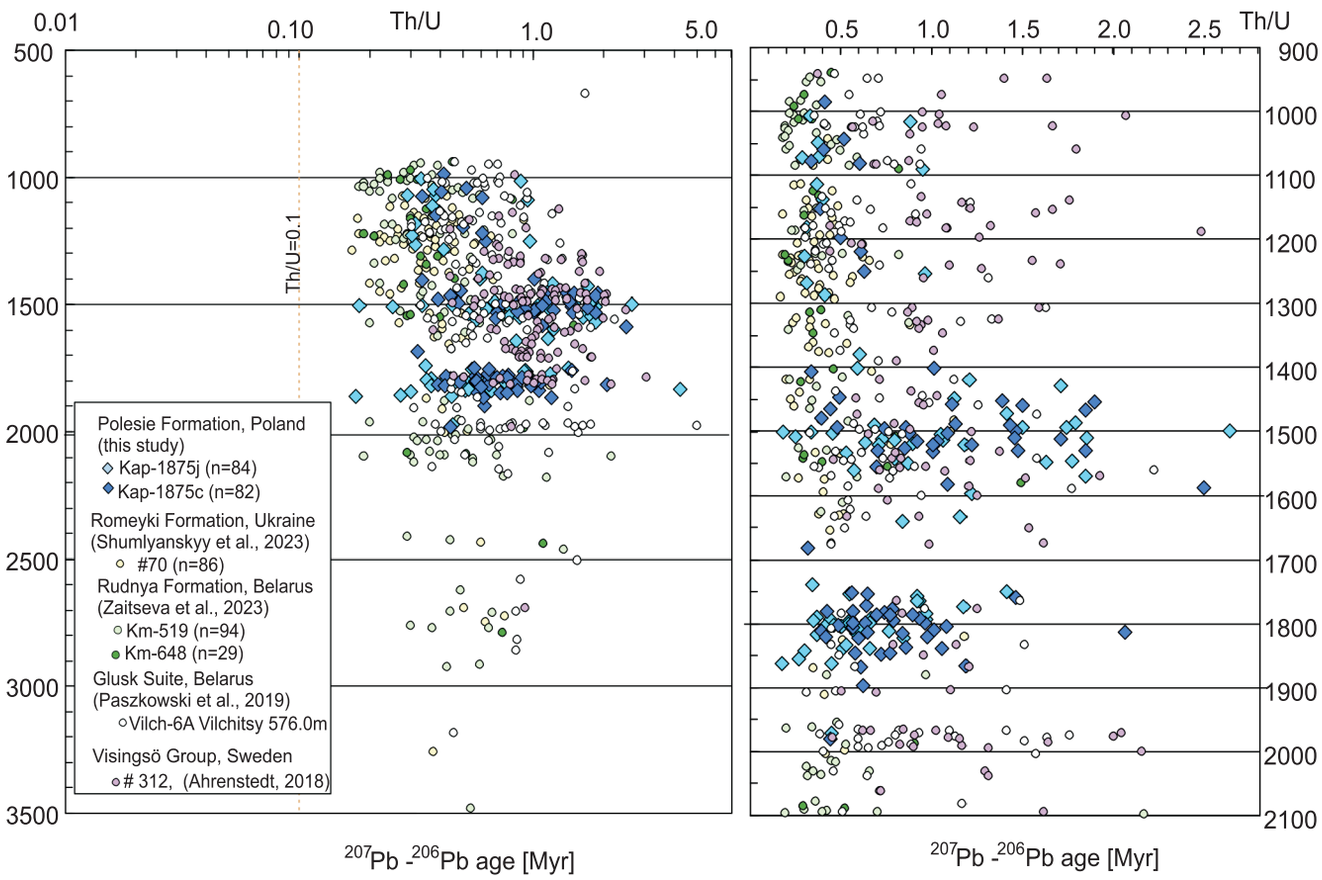

Fig. 9. Comparisons of detrital zircon ages and Th/U parameter based on data from this study and data taken from Ahrenstendt (2018); Paszkowski et al. (2019); Shumlyanskyy et al. (2023); Zaitseva et al. (2023)

(peak at 1133 ±45 Myr),. The source of these youngest zircons was the Sveconorwegian orogenic belt in the NW part of the EEC (Fig. 10), active ~1.14–0.96 Ga (Bingen et al., 2008, 2021; Bogdanowa et al., 2008; Slagstad et al., 2013). The youngest zircon grains, clustering at ~1044–1079 Myr may be regarded as of the Sveconorwegian orogen affinity, i.e., derived from the NW part of the EEC (Fig. 1) e.g. N Denmark, SW Sweden, S Norway. The Sveconorwegian orogeny at 1.15–0.9 Ga (corresponding to the Grenville orogeny in North America) amalgamated the youngest Precambrian crust to Baltica in the southwest (Bingen et al., 2008, 2021), forming ~550 km wide orogenic zone covering south Norway and southwest Sweden and one of the components of Rodinia supercontinent (Li et al., 2008). A post-orogenic relaxation was accompanied with extensional tectonism that facilitated the creation of a sedimentary basins. A subsequent processes between of the end-Mesoproterozoic and the beginning of the Neoproterozoic included a gradual peneplanation until the break-up of Rodinia at ~600 Ma. Intracratonic type basins comprise mainly Mesoproterozoic and some Neoproterozoic sediments. According to synthesis of Cawood et al. (2007) the detrital zircon record of Mesoproterozoic to early Paleozoic sedimentary successions along the eastern margin of Laurentia and Baltica are characterized by a remarkably similar pattern for ages of the main sediment pulses from the late Archaean (~2.7 Ga), late Paleoproterozoic (2.0–1.75 Ga), early Mesoproterozoic (~1.5 Ga), and late Mesoproterozoic to earliest Neoproterozoic (1.2–0.95 Ga) consistent with derivation from the cratonic interior Baltica or Laurentia.

This also applies to one of the small Neoproterozoic rift basin in southern Sweden, running NNE–SSW along the Lake Vättern consists of deltaic sandstone and marine shale, of the Visingsö Group. The recent studies of these post-Sveconorwegian sediments provided a detrital zircon age patterns of a large group of samples from a few locations (Moczydłowska et al., 2017; Ahrenstedt, 2018; Pulsipher and Dehler, 2019).

The comparison (Fig. 8) between representative sample of Visingsö Group (Ahrenstedt, 2018) and sample of Kap-1875 disclosed a very similar range of detrital zircon ages, including youngest population, however a peaks distribution shows some shifts. The age groups from Visingsö are present throughout the region of the central Sweden and can be tied to several specific stages of Svecofennian belt (2.0–1.75 Ga), the Transscandinavian igneous belt TIB (~1.86–1.66 Ga), the Gothian orogeny (1.66–1.52 Ga), Hallandian event (1.47–1.38 Ga), the Eastern Segment and Idefjorden regions (1.21–1.37 Ga), the Telemarkia Terrane (1.16 Ga) and the Sveconorwegian orogeny (1.14–0.90 Ga), indicating derivation from sources in the relative vicinity of the basin (Ahrenstedt, 2018). Also for other samples of Visingsö Group within Baltica source was concluded (Ahrenstedt, 2018; Pulsipher and Dehler, 2019).

Despite age similarity, the comparison of VOR detrital zircon dataset (Fig. 9) using the Th/U vs age diagram suggests a subtle differences of Th/U values between coeval zircons. They may indicate (1) method dependent bias (i.e. La-ICP MS vs. SHRIMP analysis) or (2) a real differences of the melt characteristics suggesting that the source rocks were coeval but not the same, although some projections in each age group over-

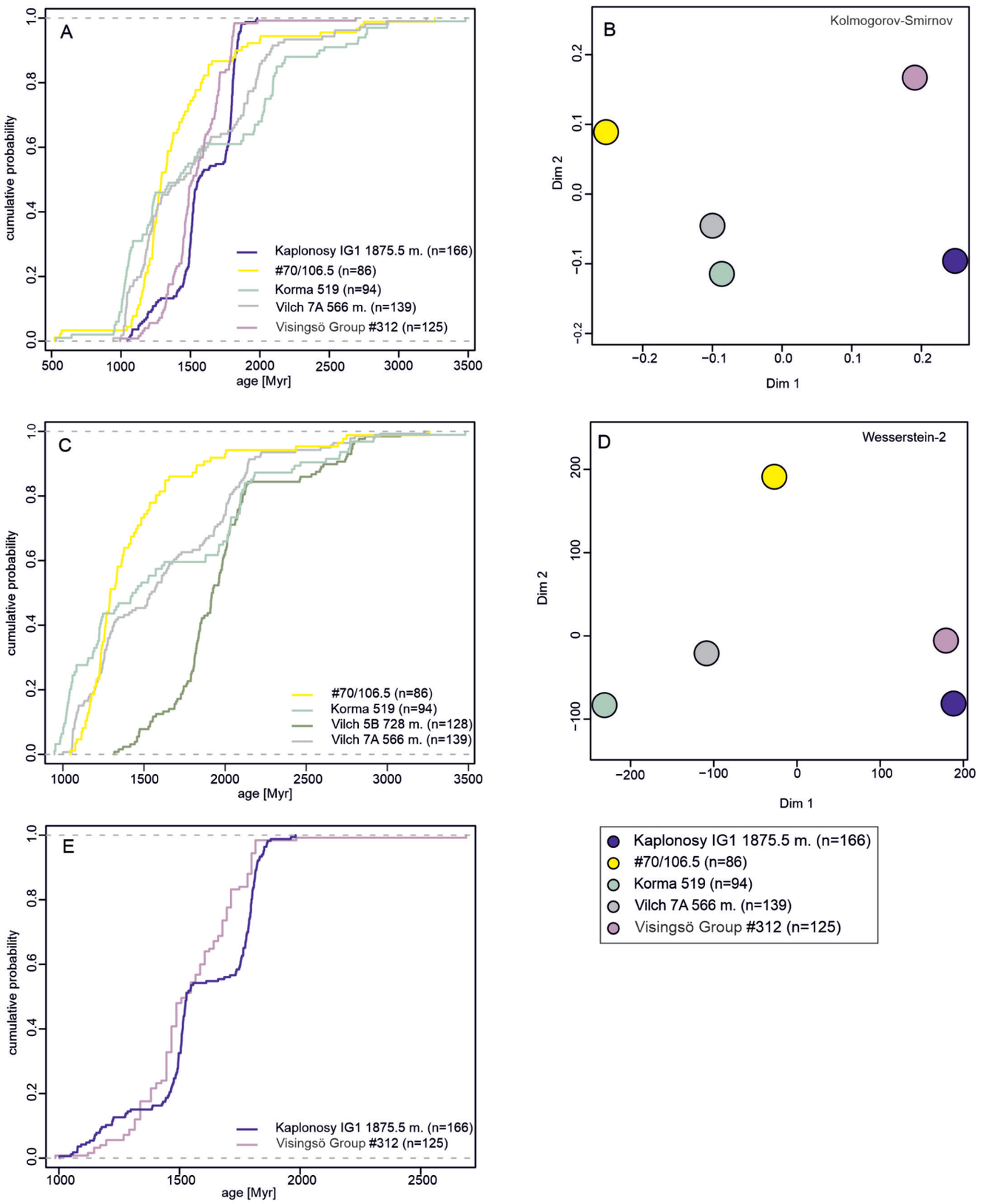

Fig. 10. Cumulative age distribution and associated multidimensional scaling (MDS) plots of detrital zircon age spectra characterizing compared samples deposited within VOR and central southern Sweden

Data taken from Ahrenstendt (2018); Paszkowski et al. (2019); Zaitseva et al. (2023); Shumlyanskyy et al. (2023)

lap. Moreover a most Kap-1875.5 zircons exhibited Th/U ratios >0.3, supporting the assertion that detrital grains have an igneous origin, consistent with the CL findings (Fig. 5). The fluctuated Th/U ratios in Kap.-1875.5 zircons exhibit a general trend of increase during 1600–1500 Ma (consistent with AMCG type source), which is followed by a decrease of youngest cluster.

The range of ~1.2–0.90 Ga, has become a characteristic indicator of the crust formed during Sveconorwegian or / and Grenvillian orogeny within the belt (Fig. 10), developed upon the continent-continent collisions related to the assembly of the supercontinent Rodinia. Thus for late Mesoproterozoic zircon age component reported from the eastern part of VOR the Grenvillian orogen (1250–980 Ma) or/and Sveconorwegian (1140–960 Ma) has been discussed as a potential source area (Shumlyanskyy et al., 2023; Zaitseva et al., 2023).

Detrital zircons from the Polesie formation contain only a small population yielding $^{207}Pb/^{206}Pb$ ages of ~1290–1050 Myr (Figs. 6 and 7E, F), but they are much common for the samples representing Polytsi Formation lateral equivalents of the Polesie formation in Ukraine (Figs. 7C, D and 10; Shumlyanskyy et al., 2015, 2023) and Rudnya Formation in the Orsha sub-basin or Pinsk Formation in Volyn-Polesie sub-basin in the Belarus (Figs. 7A, B and 10; Zaitseva et al., 2023).

The Visingsö Group sediments deposited closest to the potential source area (e.g., Sveconorwegian orogenic belt), the detrital zircons of ~1250–950 Myr are most abundant in the lower part formation (Moczydłowska et al., 2017).

CHARACTERIZING POPULATIONS HETEROGENEITY

The observed detrital zircon age spectra are influenced by proportion of zircons available in the source area for incorporation into basinal deposits and the efficiency of erosion. Although the probablity plots and histograms (Figs. 6–8) can indicate a main crustal forming events, which provided a detrital material from eroded rocks, it is difficult to properly visualize the proportions within different age groups. Therefore, a cumulative probability plots (CPPs) are introduced in this study (Fig. 11A, C, E). They allow by percentiles to compare different data distributions. Proximity between CPP or overlapping of lines implies similar detrital zircon age populations, suggesting a common source for the zircons. However a review of available detrital zircon ages from the VOR basin (Paszkowski et al., 2019; Shumlyanskyy et al., 2023; Zaitseva et al., 2023) and Visingsö post-Sveconorwegian basin (Ahrenstedt, 2018) on the CPPs diagram highlight a differences in proportions of detrital ages distribution, including that between from the Volhynian and Orsha zones of the VOR (i.e. Korma-519, Vilchi vs. #70/106.5) previously concluded by Shumlyanskyy et al. (2023).

Compared data shows a strong similarity of detrital zircon age distribution of the Orsha sediments (samples Vilch and Korma-519). This independently confirms a leading input of the same detrital material, that was available in the eroded proximal basement. The (CPPs) samples reveal two distinct curve groups (Fig. 11C vs. E), one of which represents the input of detritus from the crust of the western Sarmatia (Fig. 11C) but the other (Fig. 11E) from the central and southern Fennoscandia.

To further confirm the division observed in the CPPs two-dimensional MDS diagrams (Fig. 11B, C) of statistical metrics like the Kolmogorov-Smirnov (K-S) and Wesserstein-2 (W-2) were applied. The MDS plots capture the relative differences of populations. They are rather intuitive for visualizing the relationship between the detrital age distributions, where greater distances between sample plots represented a greater degree of dissimilarity between them. The K-S is defined as the maximum vertical distance between two empirical cumulative distribution functions, but the W2 distance is a function of the horizontal distances (i.e. age differences) between analyses set of samples.

The MDS diagram for all detrital zircon ages (Fig. 11A) shows that (1) the detrital zircon population of Korma-519 is very similar to that of the Vilchic siliciclastic rocks, both belonging to Orsha Zone; (2) there is a similarity between the Kap-1875.5 of the Polesie formation and the Visingsö Group detrital zircon populations; and (3) there is a certain degree of dissimilarity between the above pairs.

The #70 clastic rock being linked to Volynian zone shows a tenuous connection with both siliciclastic rocks groups. Both the Kolmogorov-Smirnov (K-S) Test and Wesserstein-2 Test (Fig. 11B, D) produce an analogous record of sample dissimilarity, supporting the indications identified by other diagrams, that provenance for the clastic rocks deposited within the VOR can be as different as the nearest eroded basement units (including available detritus on this basement).

All samples are characterized by multimodal patterns with grain contributions from a broader age range, including shifts towards older age components, that is characteristic for divergent/passive margin settings (Cawood et al., 2012).

CHARACTERIZING A MAXIMUM DEPOSITION AGE VERSUS YOUNGEST DETRITAL ZIRCON GRAINS

Presented detrital zircon dataset and their MDS models used here represent: (1) shales and siltstones deposits of the Visingsö Group that belong to the Neoproterozoic (i.e., Tonian) beds, as defined by microfossils that provided a minimum age of ~740 Myr (Moczydłowska et al., 2017); sedimentologically they are consistent with the few remaining evidences from this time period in Sweden, and (2) the VOR basin sediments of the Polesie formation with unknown deposition age, but considered previously as a possibly lower Stenian (1.2–1.0 Gyr) age (Bogdanova et al., 2008).

For expected stratigraphic correlation (Fig. 12) between different sampling sites (Fig. 1) within a single sedimentary basin or different basins, the age of deposition remains a most important and critical parameter. A youngest cluster of detrital zircon U-Pb dataset is routinely used to approximate an age of deposition as a so called maximum depositional age (MDA). There are at least three methods of calculating the MDA (Dickinson and Gehrels, 2009) using U-Pb ages. The most common are based on calculated ages of either the youngest single grain (YSG), the youngest grain cluster composed of three or more grains that overlap at 2 (YGC 2), using the weighted mean age of the youngest (n>3) zircons with ±2 age overlap, or concordia age as well as the youngest graphical peak (YPP). However, as has been recently emphasized by numerous works (Gehrels, 2014; Coutts et al., 2019; Sharman and Malkowski, 2020), that MDA detrital zircon may be older, even much older, than the true depositional age (TDA), usually in the passive or and amagmatic setting. This is because passive margins do not have a strong component of syndepositional magmatic activity. In case of the VOR tectonic context i.e. Rodinian intracratonic/rift and passive margin basin (see Cawood et al., 2007) the use of the youngest zircons from obtained data set as a MDA limit is rather impermissible. It may contribute to misinterpretation (Andersen, 2005). In the intracratonic basins, characterized by a lack input from syndepositional magmatic activity, resulting in an increasing gap between a real age of sediment accumulation and the youngest detrital grain.

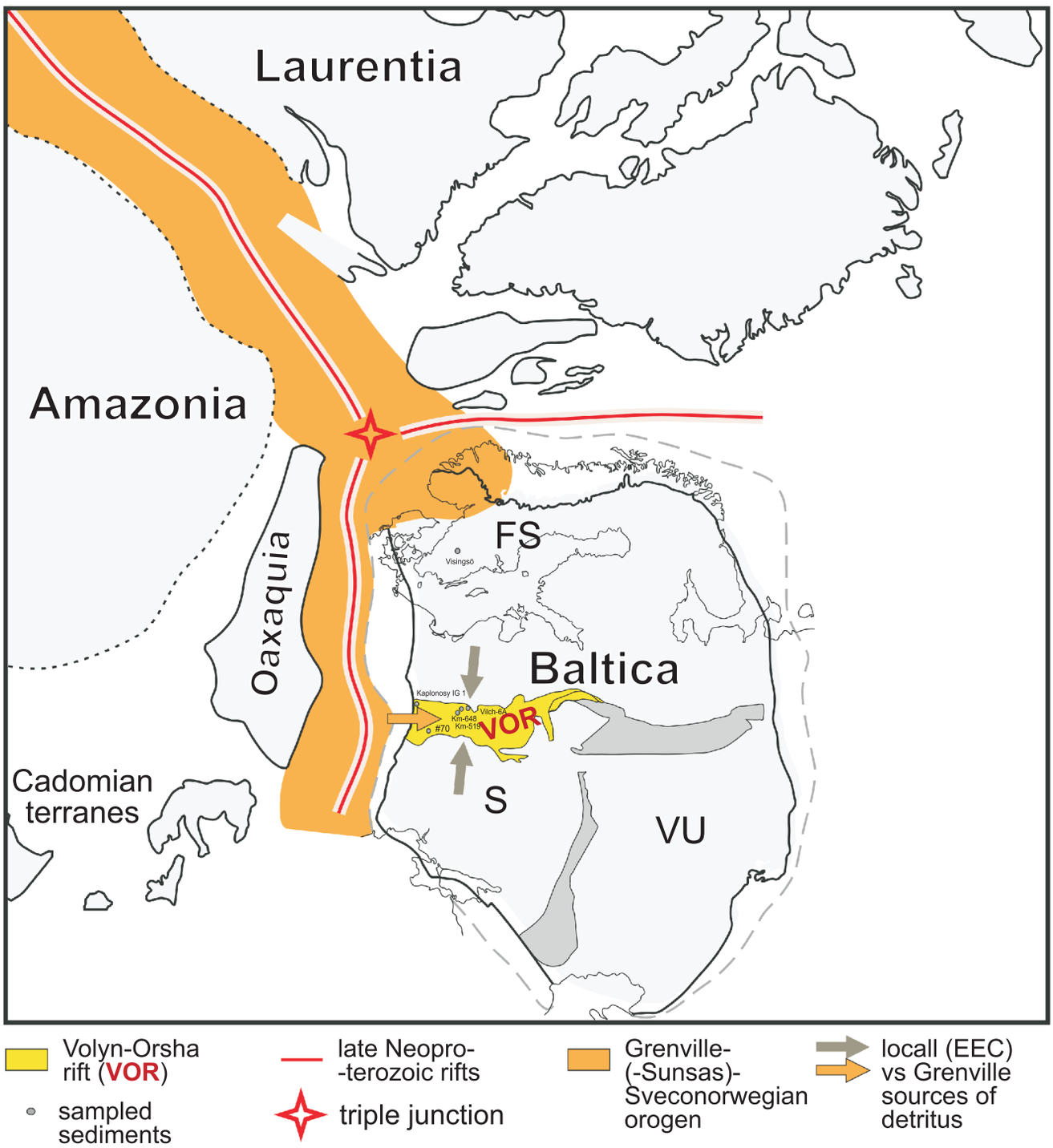

Fig. 11. Supposed palaeogeographic position of source areas of detritus for the Polesie formation relative to the position of the Orsha-Volyn Rift

The basin was supplied with detritus from both the Grenville-Sunas-Sveconorwegian orogen to the west of the Baltica, and the local cratonic sources. FS – Fennoscandia, S – Sarmatia, VU – Volgo-Uralia blocks

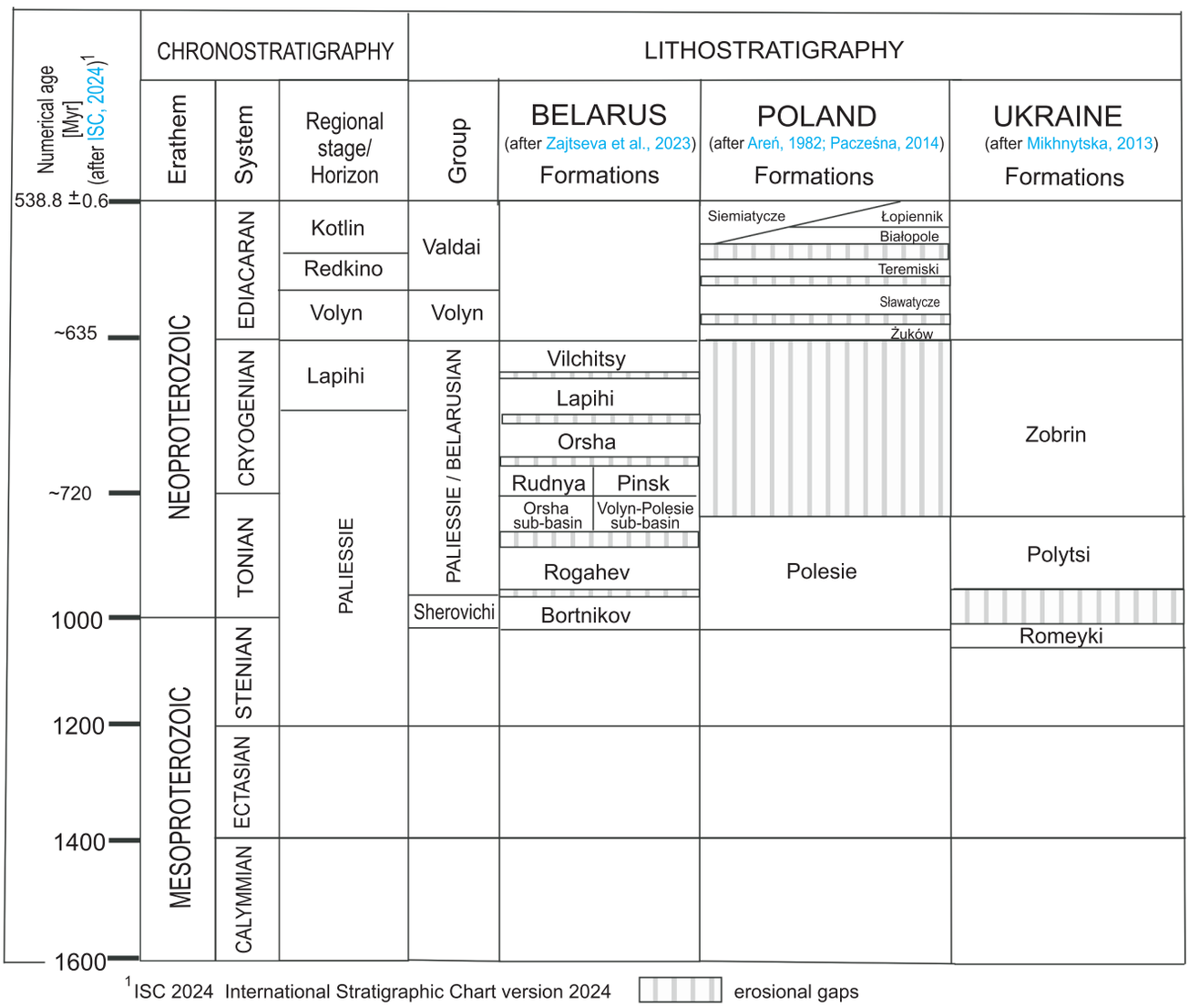

Fig. 12. Correllative scheme of the regional stratigraphical units in the Belarusian, Polish and Ukrainian part of the Volyn-Orsha Rift basin

The importance of this problem i.e. using youngest zircons to constrain the TDA within intracratonic setting may be explained by case studies of sediments from the central Fennoscandia, preserved as down faulted remnants within the vicinity of the Lake Vättern basin in southern Sweden (Fig. 1), known as the Visingsö Group. The detrital zircon provenience study from several samples and locations (Moczydłowska et al., 2017; Ahrenstedt, 2018; Pulsipher and Dehler, 2019) in this exceptional case was supported by biostratigraphic dating. A comparison of both the age cathegories reveals a difference of at least 100–150 Myr between the youngest detritus and the biostratigraphic age of the strata. U-Pb detrital zircon study by Moczydłowska et al. (2017) reported a youngest zircons as MDA of 886 ±9 Myr. The studies of another sandstones of the Visingsö Group sampled on the eastern shore of Lake Vättern (Pulsipher and Dehler, 2019) provided youngest ages in range from 941 ±12 to 1227 ±31 Myr (based on n=5 youngest grains per sample) or 919.4 ±25.1 to 1197.2 ±22.2 Myr (based on youngest single grain per sample). The upper range together with the middle Visingsö Group defined on microfossils (acritarchs of the *Cycliocyrillium simplex* assemblage) indicates the time span of ~788–740 Ma (Moczydłowska et al., 2017), which shows a gap of at least 140–150 Myr between youngest zircon grains and biostratigraphic indications. Consequently, by combining the age obtained by U-Pb dating of younger detrital zircons with the minimum age obtained from biochronological results, the deposition age was constrained to a broad range of 146 Myr between 886–740 Ma (Moczydłowska et al., 2017).

U-Pb SHRIMP dating on detrital zircons of Kap-1875.5 m (Figs. 6 and 7) allowed to recognize a youngest detrital cluster in the westernmost part of the VOR at ~1073 Myr to 1044 Myr. The youngest detrital zircon clusters of n=3 grains from the sample Korma-519 (Zaitseva et al., 2023) yielding a concordia age of 952 ±10 Myr.

The ages of 977±6 Myr and 1056 ±4 Myr (defined as MDA) have been constrained for samples Vilch-6A and Vilch-7A, respectively (Paszkowski et al., 2019), represented the Orsha Suite and Vilchitsy Series. They are somewhat younger to that result from sample #70), i.e. the weighted mean age of 1079 ±8 Myr was explained as deposition age but finally the MDA was concluded in range ~1000–950 Ma (Shumlyanskyy et al., 2023).

The sandstones of the Sherovichi series in Belarus (Fig. 12) contain a relatively large amount of zircon grains from 948 to 1030 Myr in age (Korma-519) but other nearby ones don't. These differences were explained by the complex block structure of the palaeotrough bottom, which influenced the ways of transport of terrigenous material (Zaitseva et al., 2023). In the Visingsö Group, Southern Sweden, where more samples from one sedimentary sequence was investigated the stratigraphically lowest sample contained a youngest zircons. This illogical pattern in case of the deltaic sandstone and marine shale, debris-flow marine sandstone may indicate either (i) increasingly older rockswere being unroofed and eroded, or (ii) an expanding depositional system covered younger, more locally derived material with older, more distal detritus (Moczydłowska et al., 2017) or/and deposition in a tectonically dynamic intercontinental basin (Pulsipher and Dehler, 2019).

The sediments from several locations within the VOR (Fig. 1) undoubtedly differ in the abundance of the youngest group. A representative pie charts are introduced in Figure 13 to depict the percentage for different age groups, including those related to Sveconorwegian/Grenvilian sources.

This set of diagrams indicates a relatively poor population of only 12.5% of the oldest zircons recognized in this group in Kap-1875.5 sample of Polesie formation (Fig. 13). These results from cratonic sandstones of lower part of deposits (Fig. 12) implying an input of slightly younger material, than in Kap-1875.5 sample but not mark out the TDA for the each of them.

The lag time between zircon crystallization and deposition related to amagmatic tectonic setting (Cawood et al., 2012) however does not allow for precise recognition of the real maximum age of deposition (MDA) or/and precise correlation different sampling sites. The observed variations in detrital zircon age spectra relatively well-correlate with the geological heterogeneity of the local basement, within distinct parts of the VOR. However, low-n single grains datasets compared here still remain not fully decisive. It has been recently emphasized (Zametzer et al., 2025), that detrital zircon age variations fall within typical facies variability at a single stratigraphic level when analyzing ~240 grains, but fall within the typical variability of geological formations when analyzing only ~70 grains using a representative selection strategy.

STRATIGRAPHIC POSITION

The upper limit of the Polesie formation is defined by the overlying upper Ediacaran flood basalts of Sławatycze Formation or clastic sediments of Żuków Formation, presumably not older than 580 Myr (Poprawa et al., 2020; Krzemińska et al., 2022). These constraints leave a very broad time interval for deposition of the Polesie formation (>400 Myr), covering at least the lower and/or middle Neoproterozoic. This might be narrowed down by tectono-facies arguments. The development of the Volyn-Orsha basin, being a large-scale rift structure (e.g., Bogdanova et al., 1996; Poprawa and Pacześna, 2002), should fit on a regional scale with phases of extensional tectonics. In our opinion, VOR developed in a framework of the break-up of the supercontinent Rodinia, the main phase of which took place between 800 and 650 Ma (Bogdanova et al., 2008; Scotese, 2009; Kheraskova et al., 2015). Previously, the lower part of the VOR sedimentary fill was considered to be of the Ectasian (1.4 Ga–1.2 Ga) and possibly lower Stenian (1.2–1.0 Ga) age (Bogdanova et al., 2008). This was, however, based on the imprecise K-Ar and Rb-Sr dating of mafic sills cutting sedimentary rocks of the adjacent Valday/Krestsy graben (~1.3 to 1.1 Ga; Aksenov, 1998). Due to the low precision of these geochronological data, the uncertain correlation of the sedimentary fill of the Valday/Krestsy graben and VOR, and the clear incompatibility with the U-Pb detrital zircon geochronology (Shumlyanskyy et al., 2023; Zaitseva et al., 2023), the concept of the Ectasian and/or lower Stenian age of the VOR is rejected here. The Neoproterozoic age of the Polesie formation and thus the Volyn-Orsha rifting is supported by detrital mica and feldspar K-Ar ages of 815–700 Myr and whole-rock ages of 980–880 Myr (Semenenko, 1968; Makhnach et al., 1976; Chebanenko et al., 1990). Due to these constraints on the maximum deposition age, the age of the sedimentary fill of the VOR was tentatively assigned to the late Cryogenian or Ediacaran (Poprawa, 2006).

The Precambrian continental sandstone and mudstone of the red beds type of Polesie formation, which is the sedimentary fill of the Polish part of the western Volyn-Orsha Rift basin contains no stratigraphic indexes, therefore its age remained poorly defined for a long time. Our study on U-Pb SHRIMP geochronology of detrital zircons from lowermost part of this formation brings new and strong constraints towards to its deposition time. The $^{207}Pb/^{206}Pb$ ages of the youngest zircons cluster at 1060 Myr to 1073 Myr. The youngest detrital grains define the c.a. of ~1067 ±16 Myr. The extensional tectonic regime governing the development of the Volyn-Orsha Rift is related here to the Neoproterozoic break-up of the supercontinent Rodinia (Cawood et al, 2007). Its main phase took place between 800 and 650 Ma (Bogdanova et al., 2008; Scotese, 2009; Kheraskova et al., 2015). The new observations (Callegari et al., 2023) from northern Sweden (Seve Nappe Complex) provided recently a critical age record of the Early Neoproterozoic (Tonian) break-up event manifested by metagabbro, metagranite, which coupled with bulk rock major and trace element geochemistry, suggests an unsuccessful rifting across Rodinia at 870–830 Ma. This event indicates continental-scale tectonic extension. It cannot be ruled out that the Volyn-Orsha early rifting might be of similar age, because in the intracratonic extensional to rift basins, with a lack of syn-depositional magmatic activity, the gap between a real age of sediment deposition and the youngest detrital grains cluster, increases. The Polesie formation is, therefore, younger than ~1 Gyr, while due to the age of overlying strata, it is older than 580 Myr, and is interpreted here as of the lower and/or middle Neoproterozoic age.

CONCLUSIONS

The Precambrian continental sandstone and mudstone of red beds type of the Polesie formation, which is the sedimentary fill of the Polish part of the intracratonic VOR basin, contains no biostratigraphic indexes. The U-Pb dating of detrital zircons of the lowermost deposits (Kap-1875.5m) of the western sub-basin reflect the erosional unroofing history of the adjacent late Svecofennian orogenic and AMCG related suites.

Our study on U-Pb SHRIMP geochronology of detrital zircons from this formation brings new constraints on its time of deposition age based on youngest grains.

The youngest (n=3) detrital zircons define an age of ~1067 ±16 Myr (c.a.), interpreted as pre-depositional in this amagmatic setting. It indicate deposition after this age as the rock must be younger than its component.

Due to the intracratonic position of VOR basin where the gap between age of sediment accumulation and the youngest detrital grain occurs and the newly recognized age of the youngest detrital zircon cluster (1067 ±16 Myr), the late Mesoproterozoic stratigraphic position is questioned.

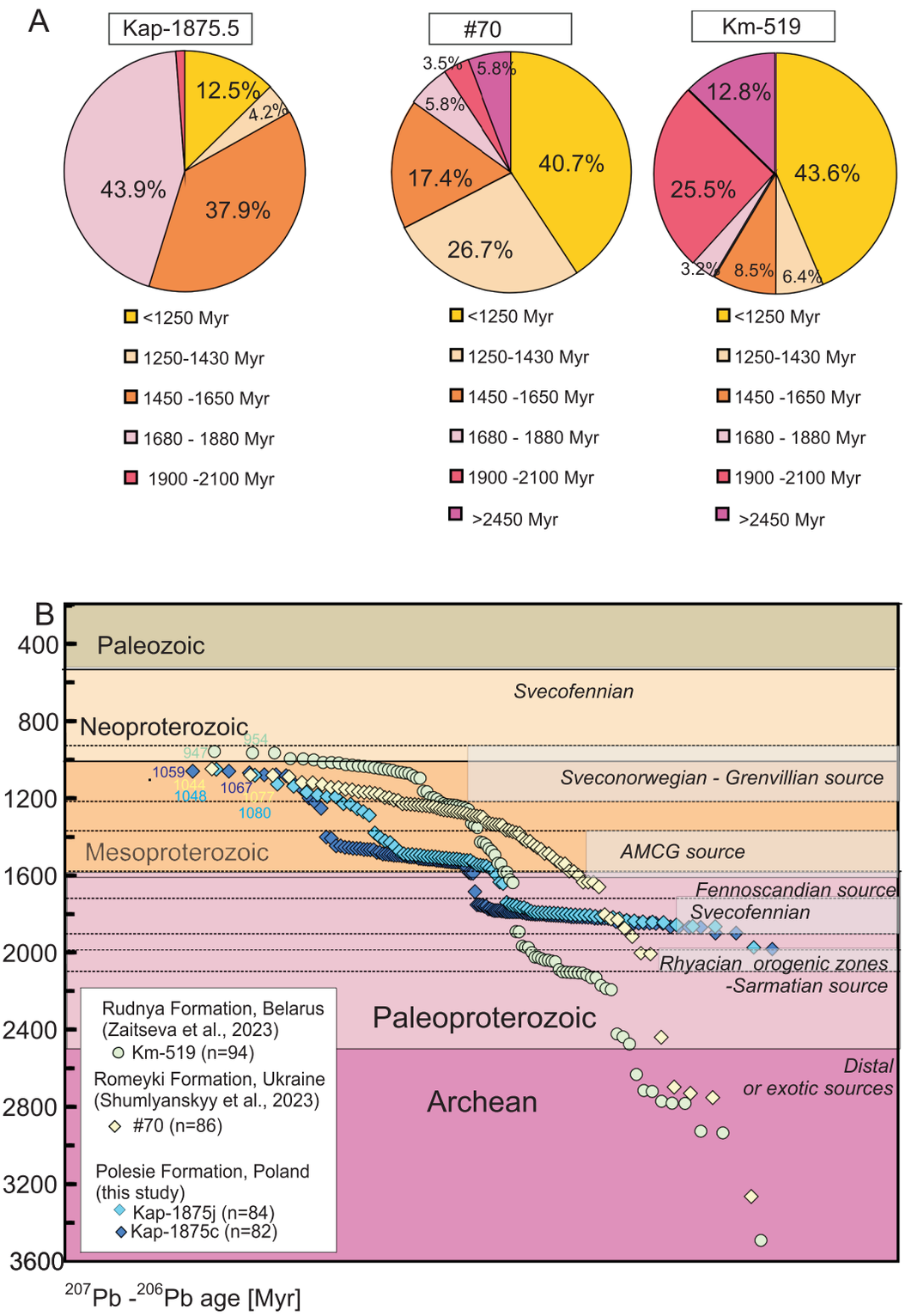

Fig. 13. Schematic diagram including a comparison of detrital zircon ages of the early Neoproterozoic cratonic sandstones from lower part of VOR

A – pie chart graphics showing the proportion of the zircon Pb-Pb ages according to the time frames matched to the source areas and rocks; **B** – Linearized-probability plot diagram showing a distribution of detrital components within distinct parts of VOR; generalized potential source areas and rocks are indicated. Data after Zaitseva et al. (2023) – sample Km-519; after Shumlyanskyy et al. (2023) – sample #70; sample Kap-1875.5 merged (this study)

The development of the Volyn-Orsha Rift was governed by the extensional tectonic regime related here to the Neoproterozoic break-up of the supercontinent Rodinia. Its earliest episode of continental–scale extension took place between 870–830 or 800 Ma, thus, the Volyn-Orsha rifting might be initiated coevally. The Polesie formation is presumably, younger than ~1 Gyr, while due to the age of overlying strata, it is older than 580 Myr, and is interpreted here as of the early and/or middle Neoproterozoic age.

The main source of detritus in the western part of the VOR was located to the north and north-west of the basin. This is represented by the two major populations of zircon grains. that yields Pb-Pb ages in a range of ~1.56–1.45 Gyr (41%) with a well-defined peak at 1500.5 ±2.5 Myr, and of ~1.85–1.75 Gyr (46% of zircon grains) with a peak at 1807 ±1.4 Myr. This detritus represents an influx of relatively proximal north westerly derived cratonic detritus originated from the anorogenic AMCG suite common in the direct vicinity of the NW margin and supplied from the denudated Svecofennian basement of the NW surrounding of the basin.

The youngest zircon grains, clustering at ~1044–1079 Myr could be regarded as of the Sveconorwegian–Grenvillian affinity, i.e. derived from the NW part of the EEC (N Denmark, SW Sweden, S Norway).

The early Neoproterozoic siliciclastic deposits from a VOR compared in this contribution revealed a different detrital zircon age patterns. The prominent feature remains a presence of the youngest detritus cluster derived from denudation of the Sveconorwegian/Grenvillian rocks. Among these youngest sources those related to the Sveconorwegian/Grenvillian source, increase from 13% in Kaplonosy sedimentary rock (E Poland) to more than 40% in #70 sandstone sample (W Ukraine) and to 43.6% in Korma sandstone sample (W Belarus), which reach a dominant percentages comparable to the Svecofennian source (43%) in E Poland.

These results determine not only the differences in the proximal source of detrital material, i.e. distinct local basement, but most likely reflect progressive shift or greater influence of the Sveconorwegian-Grenvillian material.

Acknowledgements. The analytical works were financially supported by the Polish Geological Institute – National Research Institute (PGI–NRI) internal grant number 62.9012.2165.00.0. The contribution of Paweł Poprawa was supported by the AGH-KSE Statutory Fund 16.16.140.315/05. We thank Jarosław Majka and an anonymous referee for all constructive comments and suggestions, which greatly inspired to improve the manuscript.

REFERENCES

Ahrenstedt, V., 2018. The Neoproterozoic Visingsö Group of southern Sweden: lithology, sequence stratigraphy and provenance of the Middle Formation. Dissertations in Geology at Lund University, **551**.

Aksenov, E.M., 1998. The Geological Evolution of the East European Craton in the Late Proterozoic (in Russian). Institute of Precambrian Geology and Geochronology, Summary of Ph.D. thesis, St. Petersburg, Russia.

Andersen, T., 2005. Detrital zircons as tracers of sedimentary provenance: limiting conditions from statistics and numerical simulation, Chemical Geology, **216**: 249–270; https://doi.org/10.1016/j.chemgeo.2004.11.013

Areń, B., 1982. Lithological-facies development of the Upper Vendian in eastern Poland area (in Polish with English summary). Przegląd Geologiczny, **30**: 225–230.

Bibikova, E.V., Bogdanova, S.V., Postnikov, A.V., Popova, L.P., Kirnozova, T.I., Fugzan, M.M., Glushchenko, V.V., 2009. Sarmatia–Volgo-Uralia Junction Zone: Isotopic-Geochronologic Characteristic of Supracrustal Rocks and Granitoids. Stratigraphy and Geological Correlation, **17**: 561–573; https://doi.org/10.1134/S086959380906001X

Bingen, B., Andersson, J., Söderlund, U., Möller, C., 2008. The Mesoproterozoic in the Nordic countries. Episodes, **31**: 29–34; https://doi.org/10.18814/epiiugs/2008/v31i1/005

Bingen, B., Viola, G., Möller, C., Vander Auwera, J., Laurent, A., Yi, K., 2021. The Sveconorwegian orogeny. Gondwana Research, **90**: 273–313; https://doi.org/10.1016/j.gr.2020.10.014

Black, L.P., Kamo, S.L., Allen, C.M., Aleinikoff, J.A., Davis, D.W., Korsch, J.R., Foudolis, C., 2003. TEMORA 1: a new zircon standard for Phanerozoic U-Pb geochronology. Chemical Geology, **200:** 155–170; https://doi.org/10.1016/S0009-2541(03)00165-7

Bogdanova, S.V., Pashkevich, I.K., Gorbatschev, R., Orlyuk, M.I., 1996. Riphean rifting and major Palaeoproterozoic crustal boundaries in the basement of the East European Craton: geology and geophysics. Tectonophysics, **268**: 1–21; https://doi.org/10.1016/S0040-1951(96)00232-6

Bogdanova, S., Gorbatchev, R., Grad, M., Janik, T., Guterch, A., Kozlowskaya, E., Motuza ,G., Skridlaite, G., Starostenko, I., Taran, L., Eurobridge and Polonaise working Group 2006. EUROBRIDGE: new insight into the geodynamic evolution of East European craton. Geological Society Memoirs, **32**: 599–625.

Bogdanova, S.V., Bingen, B., Gorbatschev, R., Kheraskova, T.N., Kozlov, V.I., Puchkov, V.N., Volozh, Y.A., 2008. The East European Craton (Baltica) before and during the assembly of Rodinia. Precambrian Research, **160**: 23–45; https://doi.org/10.1016/j.precamres.2007.04.024

Bogdanova, S.V., Gorbatschev, R., Skridlaite, G., Soesoo, A., Taran, L., Kurlovich, D., 2015. Trans-Baltic Palaeoproterozoic correlations towards the reconstruction of supercontinent Columbia/Nuna. Precambrian Research, **259**: 5–33; https://doi.org/10.1016/j.precamres.2014.11.023

Callegari, R., Kośmińska, K., Barnes, C., Klonowska, I., Barker, A., Rousku, S., Nääs, E., Kooijman, E., Witt-Nilsson, P., Majka, J., 2023. Early Neoproterozoic magmatism and Caledonian metamorphism recorded by the Mĺrma terrane, Seve Nappe Complex, northern Swedish Caledonides. Journal of the Geological Society, **180**, jgs2022-092; https://doi.org/10.1144/jgs2022-092

Cawood, P.A., Nemchin, A.A., Strachan, R., Prave, A., Krabbendam, M., 2007. Sedimentary basin and detrital zircon record along East Laurentia and Baltica during assembly and breakup of Rodinia. Journal of the Geological Society, **164**: 257–275; https://doi.org/10.1144/0016-76492006-115

Cawood, P.A., Hawkesworth, C.J., Dhuime, B., 2012. Detrital zircon record and tectonic setting. Geology, **40**: 875–878; https://doi.org/10.1130/G32945.1

Chebanenko, I.I., Vyshnyakov, I.B., Vlasov, B.I., 1990. Geotectonics of the Volyno-Podolian area (in Russian). Naukova Dumka, Kiev.

Coutts, D.S., William, A.M., Stephen, M.H., 2019. Assessment of widely used methods to derive depositional ages from detrital zircon populations. Geoscience Frontiers, **10:** 1421–1435; https://doi.org/10.1016/j.gsf.2018.11.002

Dadlez, R., Marek, S., 1997. Development of Permian and Mesozoic basins (in Polish with English summary). Prace Państwowego Instytutu Geologicznego, **153**: 403–409.

Dickinson, W.R., Gehrels, G.E., 2009. Use of U–Pb ages of detrital zircons to infer maximum depositional ages of strata: a test against a Colorado Plateau Mesozoic database. Earth and Planetary Science Letters, **288**: 115–125; https://doi.org/10.1016/j.epsl.2009.09.013

Gareckij, R.G., Zinovienko, G.V., Visnjakov, I.B., Glusko, V.V., Pomjanovskaja, G.M., Lvov, G.M., 1987. Die perikratone Baltik-Dnestr-Senkungszone. Zeitschrift für angewandte Geologie, **33**: 207–213.

Gehrels, G., 2014. Detrital zircon U–Pb geochronology applied to tectonics. Annual Review of Earth and Planetary Sciences, **42:** 127–149; https://doi.org/10.1146/annurev-earth-050212-124012, 2014

Grabarczyk, A., Wiszniewska, J., Krzemińska, E., Petecki, Z., 2023. A new A-type granitoid occurrence in southernmost Fennoscandia: geochemistry, age and origin of rapakivi-type quartz monzonite from the Pietkowo IG1 borehole, NE Poland. Mineralogy and Petrology, **117**: 1–25; https://doi.org/10.1007/s00710-022-00799-7

Jaworowski, K., 1997. Depositional environments of the Lower and Middle Cambrian sandstone bodies (in Polish with English summary). Biuletyn Państwowego Instytutu Geologicznego, **377**: 1–118.

Johansson, Å., Bingen, B., Huhma, H., Waight, T., Vestergaard, R., Soesoo, A., Skridlaite, G., Krzeminska, E., Shumlyanskyy, L., Holland, M.E., Holm-Denoma, C., Teixeira, W., Faleiros, F.M., Ribeiro, B.V., Jacobs, J., Wang, C., Thomas, R.J., Macey, P.H., Kirkland, C.L., Hartnady, M.I.H., Eglington, B.M., Puetz, S.J., Condie, K.C., 2022. A geochronological review of magmatism along the external margin of Columbia and in the Grenville-age orogens forming the core of Rodinia. Precambrian Research, **371**, 106463; https://doi.org/10.1016/j.precamres.2021.106463

Juskowiakowa, M., 1974. The youngest Precambrian (in Polish). Prace Instytutu Geologicznego, **74**: 24–26.

Kheraskova, T.N., Volozh, Y.A., Antipov, M.P., Bykadorov, V.A., Sapozhnikov, R.B., 2015. Correlation of late Precambrian and Paleozoic events in the East European Platform and the adjacent paleooceanic domains. Geotectonics, **49**: 27–52; https://doi.org/10.1134/S0016852115010021

Krzemińska, E., Krzemiński, L., Petecki, Z., Wiszniewska, J., Salwa, S., Ýaba, J., Gaidzik, K., Williams, I.S., Rosowiecka, O., Taran, L., Johansson, Å., Pécskay, Z., Demaiffe, D., Grabowski, J., Zieliński, G., 2017. Geological Map of Crystalline Basement in the Polish Part of the East European Platform 1: 1 000 000. Polish Geological Institute – NRI, Warsaw.

Krzemińska, E., Krzemiński, L., Poprawa, P., Pacześna, J., Nejbert, K., 2021. First evidence of the post-Variscan magmatic pulse on the western edge of East European Craton: U-Pb geochronology and geochemistry of the dolerite in the Lublin Podlasie basin, eastern Poland. Minerals, **11**, 1361; https://doi.org/10.3390/min11121361

Krzemińska, E., Poprawa, P., Pacześna, J., Krzemiński, L., 2022. From initiation to termination: The evolution of the Ediacaran Volyn large igneous province (SW East European Craton) constrained by comparative geochemistry of proximal tuffs versus lavas and zircon geochronology. Precambrian Research, **370**, 106560; https://doi.org/10.1016/j.precamres.2022.106560

Krzemińska, E., Pacześna, J., Poprawa, P., 2024. Detrital zircon Pb-Pb dating of the Polesie Formation – provenance and maximum deposition age of the oldest sediments at the western slope of the East European Craton (Orsha-Volyn rift, SE Poland). Mineralogia, Special Papers, **52**: 67.

Krzemińska, E., Krzemiński, L., Demaiffe, D., Poprawa, P., Williams, I.S., Wiszniewska, J., 2025. Evidence of magmatic versus hydrothermal zircon ages and mantle-crust interactions obtained from the Carboniferous alkaline intrusions at the margin of East European Craton (NE Poland). Gondwana Research, **142**: 44–72; https://doi.org/10.1016/j.gr.2025.01.017

Li, Z.X., Bogdanova, S.V., Collins, A.S., Davidson, A., De Waele, B., Ernst, R.E., Fitzsimons, I.C.W., Fuck, R.A., Gladkochub, D.P., Jacobs, J., Karlstrom, K.E., Lu, S., Natapov, L.M., Pease, V., Pisarevsky, S.A., Thrane, K., Vernikovsky, V., 2008. Assembly, configuration, and break-up history of Rodinia: a synthesis. Precambrian Research, **160**: 179–210.

Ludwig, K.R., 2003. Isoplot 3.00. A Geochronological Toolkit for Microsoft Excel. Berkeley Geochronology Center, Berkeley.

Ludwig, K.R., 2008. Isoplot/Ex 3.70. A Geochronological Toolkit for Microsoft Excel. Berkeley Geochronological Center, Berkeley, CA, USA, Special Publication, **4**.

Ludwig, K.R., 2009. SQUID 2.50. A User's Manual. Berkeley Geochronology Centre, CA, USA, Special Publication, **5**; https://sourceforge.net/projects/squid2

Makhnach, A.S., Veretennikov, N.V., Shkuratov, V.I., Bordon, V.E., 1976. Riphean and Vendian of Belarus (in Russian). Nauka i Tekhnika, Minsk.

Makhnach, A.S., Garetskiy, R.G., Matvieyeva, A.W., 2001. Geology of Belarus (in Russian). Belarussian National Academy of Sciences, Institute of Geological Sciences, Minsk.

McIntyre, G.A., Brooks, C., Compston, W., Turek, A., 1966. The statistical assessment of Rb-Sr isochrons. Geophysical Research, **71**: 5459–5468; https://doi.org/10.1029/JZ071i022p05459

Mikhnytska, T.P., 2013. Stratigraphy of Riphean (in Ukrainian). In: Stratigraphy of upper Proterozoic and Phanerozoic of Ukraine (ed. P.F. Gozhyk), **1**: 31–46. Institute of Geological Sciences. NANU, Kyiv.

Miłaczewski, L., 1981. Devonian of the southeastern Lublin region (in Polish with English summary). Prace Instytutu Geologicznego, **101**.

Miłaczewski, L., Radlicz, K., 1974. Devonian (in Polish with English summary). Prace Instytutu Geologicznego, **74**: 83–98.

Moczydłowska, M., 1991. Acritarch biostratigraphy of the Lower Cambrian and the Precambrian-Cambrian boundary in southeastern Poland. Fossils and Strata, **29**: 1–127.

Moczydłowska, M., Pease, V., Willman, S., Wickström, L. Agić, H., 2017. A Tonian age for the Visingsö Group in Sweden constrained by detrital zircon dating and biochronology: implications for evolutionary events. Geological Magazine, **155**: 1175–1189; https://doi.org/10.1017/S0016756817000085

Modliński, Z., 1982. The Development of Ordovician Lithofacies and Palaeotectonics in the area of the Precambrian Platform (in Polish with English summary). Prace Instytutu Geologicznego, **52**.

Modliński, Z., Szymański, B., 2008. The Ordovician lithostratigraphy of the Podlasie Depression and the Płock-Warsaw Trough (eastern Poland) (in Polish with English summary). Biuletyn Państwowego Instytutu Geologicznego, **430**: 79–112.

Modliński, Z., Jaworowski, K., Miłaczewski, L., Pacześna, J., Podhalańska, T., Sikorska, M., Szymański, B., Waksmundzka, M.I., 2010. Paleogeological Atlas of the Sub-Permian Paleozoic of the East European Craton in Poland and Neighbouring Areas, 1 : 2 000 000. Polish Geological Institute – NRI, Warsaw.

Narkiewicz, M., Miłaczewski, L., Krzywiec, P., Szewczyk, J., 1998. Outline of the Devonian depositional architecture in the Lublin-Radom area (in Polish with English summary). Prace Państwowego Instytutu Geologicznego, **165**: 57–72.

Nosova, A.A., Kuzmenkova, O.F., Veretennikov, N.V., Petrova, L.G., Levskiy, L.K., 2008. Neoproterozoic Volyn-Brest magmatic province on western margin of the East European Craton: Peculiarities of intracratonic magmatism in the area of ancient suture zone (in Russian). Petrologia, **16**: 115–147.

Pacześna, J., 1996. The Vendian and Cambrian ichnocoenoses from the East-European Platform. Prace Państwowego Instytutu Geologicznego, **152**.

Pacześna, J., 2006. The evolution of the late Neoproterozoic-early Cambrian rift depocentres and facies in the Lublin-Podlasie sedimentary basin (in Polish with English summary). Prace Państwowego Instytutu Geologicznego, **186**: 1–29.

Pacześna, J., 2007. Busówno IG 1. Profil statygraficzny (in Polish). Profile Głębokich Otworów Wiertniczych Państwowego Instytutu Geologicznego, **118**: 9–14; 206–207.

Pacześna, J., 2010. The evolution of late Ediacaran riverine-estuarine system in the Lublin-Podlasie slope of the East European Craton (southeastern Poland). Polish Geological Institute Special Papers, **27**.

Pacześna, J., 2014. Lithostratigraphy of the Ediacaran deposits in the Lublin-Podlasie sedimentary basin (eastern and south-eastern Poland) (in Polish with English summary). Biuletyn Państwowego Instytutu Geologicznego, **460**: 1–24.

Pacześna, J., Poprawa, P., 2005. Eustatic versus tectonic control on the development of Neoproterozoic and Cambrian stratigraphic sequences of the Lublin-Podlasie Basin (SW margin of Baltica). Geosciences Journal, **9**: 117–127.

Paszkowski, M., Budzyń, B., Mazur, S., Sláma, J., Shumlyanskyy, L., Środoń, J., Dhuime, B., Kędzior, A., Liivamägi, S., Pisarzowska, A., 2019. Detrital zircon U-Pb and Hf constraints on provenance and timing of deposition of the Mesoproterozoic to Cambrian sedimentary cover of the East European Craton, Belarus. Precambrian Research, **331**, 105352; https://doi.org/10.1016/j.precamres.2019.105352

Piwocki, M., Kramarska, R., 2004. Polish Lowlands and their southern rim – basics of stratigraphy (in Polish). In: Budowa Geologiczna Polski, **1**, Stratygrafia, Część 3a, Kenozoik, Paleogen, Neogen (eds. T.M. Peryt and M. Piwocki): 19–22. Państwowy Instytut Geologiczny, Warszawa.

Poprawa, P., 2006. Neoproterozoic break-up of the supercontinent Rodiania/Pannotia recorded by development of sedimentary basins at the western slope of Baltika (in Polish with English summary). Prace Państwowego Instytutu Geologicznego, **186**: 165–188.

Poprawa, P., 2019. Geological setting and Ediacaran-Paleozoic evolution of the western slope of the East European Craton and adjacent regions. Annales Societatis Geologorum Poloniae, **89**: 347–380; https://doi.org/10.14241/asgp.2019.23

Poprawa, P., 2020. Lower Paleozoic oil and gas shale in the Baltic-Podlasie-Lublin Basin (central and eastern Europe) – a review. Geological Quarterly, **64** (3): 515–566; https://doi.org/10.7306/gq.1542

Poprawa, P., Pacześna, J., 2002. Late Neoproterozoic to Early Paleozoic development of a rift at the Lublin-Podlasie slope of the East European Craton – analysis of subsidence and facies record (in Polish with English summary). Przegląd Geologiczny, **50**: 49–61.

Poprawa, P., Šliaupa, S., Stephenson, R.A., Lazauskienė, J., 1999. Late Vendian-Early Palaeozoic tectonic evolution of the Baltic basin: regional implications from subsidence analysis. Tectonophysics, **314**: 219–239; https://doi.org/10.1016/S0040-1951(99)00245-0

Poprawa, P., Radkovets, N., Rauball, J., 2018. Ediacaran–Paleozoic subsidence history of the Volyn-Podillya-Moldova basin (Western and SW Ukraine, Moldova, NE Romania). Geological Quarterly, **62** (3): 459–486; https://doi.org/10.7306/gq.1418

Poprawa, P., Krzemińska, E., Pacześna, J., Amstrong, R., 2020. Geochronology of the Volyn volcanic complex at the western slope of the East European Craton – relevance to the Neoproterozoic rifting and the break-up of Rodinia/Pannotia. Precambrian Research, **346**, 105817; https://doi.org/10.1016/j.precamres.2020.105817

Poprawa, P., Nejbert, K., Krzywiec, P., Krzemińska, E., Krzemiński, L., Mazur, S., Słaby, E., 2024. Alkaline magmatism from the Lublin-Baltic area of Poland (SW slope of the East European Craton) – manifestation of hitherto unrecognized early Carboniferous igneous province. Terra Nova, **36**: 77–88; https://doi.org/10.1111/ter.12681

Porębski, S.J., Podhalańska, T., 2019. Ordovician–Silurian lithostratigraphy of the East European Craton in Poland. Annales Societatis Geologorum Poloniae, **89**: 95–104; https://doi.org/10.14241/asgp.2019.05

Porzycki, J., Zdanowski, A., 1995. Southeastern Poland (Lublin Carboniferous basin). Prace Państwowego Instytutu Geologicznego, **148**: 102–109.

Pulsipher, M., Dehler, C., 2019. U-Pb detrital zircon geochronology, petrography, and synthesis of the middle Neoproterozoic Visingsö Group, Southern Sweden. Precambrian Research, **320**: 323–333; https://doi.org/10.1016/j.precamres.2018.11.011

Rivers, T., 2008. Assembly and preservation of lower, mid, and upper orogenic crust in the Grenville Province – implications for the evolution of large hot long-duration orogens. Precambrian Research, **167**: 237–259; https://doi.org/10.1016/j.precamres.2008.08.00

Rivers, T., 2012. Tectonic Setting and Evolution of the Grenville Orogen: An Assessment of Progress Over the Last 40 Years. Geoscience Canada, **42**: 77–124; https://doi.org/10.12789/geocanj.2014.41.057

Scotese, C.R., 2009. Late Proterozoic plate tectonics and palaeogeography: a tale of two supercontinents, Rodinia and Pannotia. Geological Society Special Publications, **326**: 67–83; https://doi.org/10.1144/ SP326.4

Semenenko, N.P., 1968. Riphean Volcanism and Mineralization of the Western Part of the Ukrainian Shield (in Russian). Naukova Dumka, Kiev.

Sharman, G.R., Malkowski, M.A. 2020. Needles in a haystack: detrital zircon U-Pb ages and the maximum depositional age of modern global sediment. Earth-Science Reviews, **203,** 103109; https://doi.org/10.1016/j.earscirev.2020.103109

Shumlyanskyy, L., Andréasson, P.G., 2004. New geochemical and geochronological data from the Volyn Flood Basalt in Ukraine and correlation with large igneous events in Baltoscandia. GFF, **126**: 85–86.

Shumlyanskyy, L., Hawkesworth, C., Dhuime, B., Billström, K., Claesson, S., Storey, C., 2015. $^{207}Pb/^{206}Pb$ ages and Hf isotope composition of zircons from sedimentary rocks of the Ukrainian shield: Crustal growth of the south-western part of East European craton from Archaean to Neoproterozoic. Precambrian Research, **260**: 39–54; https://doi.org/10.1016/j.precamres.2015.01.007

Shumlyanskyy, L., Nosova, A., Billström, K., Söderlund, U., Andréasson, P.G., Kuzmenkova, O., 2016. The U-Pb zircon and baddeleyite ages of the Neoproterozoic Volyn Large Igneous Province: implication for the age of the magmatism and the nature of a crustal contaminant. GFF, **138**: 17–30; https://doi.org/10.1080/11035897.2015.1123289

Shumlyanskyy, L., Bekker, A., Tarasko, I., Francovschi, I., Wilde, S.A., Melnychuk, V., 2023. Detrital Zircon Geochronology of the Volyn-Orsha Sedimentary Basin in Western Ukraine: Implications for the Meso-Neoproterozoic History of Baltica and Possible Link to Amazonia and the Grenvillian-Sveconorwegian-Sunsas Orogenic Belts. Geosciences, **13**, 152; https://doi.org/10.3390/geosciences13050152

Skridlaitė, G., Siliauskas, L., Whitehouse, M.J., Johansson, Å., Rimsa, A., 2021. On the origin and evolution of the 1.86–1.76 Ga Mid-Baltic Belt in the western East European Craton. Precambrian Research, **367**,106403; https://doi.org/10.1016/j.precamres.2021.106403

Slagstad, T., Roberts, N.M.W., Marker, M., Røhr, T.S., Schiellerup, H., 2013. A non-collisional, accretionary Sveconorwegian orogen. Terra Nova, **25**: 30–37; https://doi.org/10.1111/ter.12001

Slagstad, T., Marker, M., Roberts, N.M.W., Saalmann, K., Kirkland, C.L., Kulakov, E., Ganerød, M., Røhr, T.S., Møkkelgjerd, S.H.H., Granseth, A., Sørensen, B.E., 2020. The Sveconorwegian orogeny – reamalgamation of the fragmented southwestern margin of Fennoscandia. Precambrian Research, **350**, 105877; https://doi.org/10.1016/j.precamres.2020.105877

Slagstad, T., Skår, Ø., Bjerkan, G., Coint, N., Granseth, A., Kirkland, C.L., Kulakov, E., Mansur, E., Orvik, A.A., Petersson, A., Roberts, N.M.W., 2024. Subduction and loss of continental crust during the Mesoproterozoic Sveconorwegian Orogeny. Precambrian Research, **409**, 107454; https://doi.org/10.1016/j.precamres.2024.107454

Sliaupa, S., Fokin, P., Lazauskienė, J., Stephenson, R.A., 2006. The Vendian–Early Palaeozoic sedimentary basins of the East European Craton. Geological Society Memoirs, **32**: 449–462.

Steiger, R.H., Jager, E., 1977. Subcommission on geochronology; Convention on the use of decay constants in geo- and cosmochronology. Earth and Planetary Science Letters, **36**: 359–362; https://doi.org/10.1016/0012-821X(77)90060-7

Środoń, J., Kuzmenkova, O., Stanek, J.J., Petit, S., Beaufort, D., Gilg, H.A., Liivamägi, S., Goryl, M., Marynowski, L., Szczerba, M., 2019. Hydrothermal alteration of the Ediacaran Volyn-Brest volcanics on the western margin of the East European Craton. Precambrian Research, **325**: 217–235; https://doi.org/10.1016/j.precamres.2019.02.015

Waksmundzka, M.I., 1998. Depositional architecture of the Carboniferous Lublin Basin (in Polish with English summary). Prace Państwowego Instytutu Geologicznego, **165**: 89–100.

Wang, C.C., Jacobs, J., Elburg, M.A., Läufer, A., Thomas, R.J., Elvevold, S., 2020. Grenville-age continental arc magmatism and crustal evolution in central Dronning Maud Land (East Antarctica): Zircon geochronological and Hf-O isotopic evidence. Gondwana Research, **82**: 108–127; https://doi.org/10.1016/j.gr.2019.12.004

Wichrowska, M., 1992. The Riphean deposits on the Polish platform area (in Polish with English summary). Przegląd Geologiczny, **40**: 94–99.

Wiedenbeck, M., Alle, P., Corfu, F., Griffin, W.L., Meier, M., Oberll, F., von Quadt, A., Roddick, J.C., Spiegel, W., 1995.Three natural zircon standards for U-Th-Pb, Lu-Hf, trace element and REE analyses. Geostandards Newsletter, **19:** 1–23.

Williams, I.S., 1998. U-Th-Pb geochronology by ion microprobe. Reviews in Economic Geology, **7**: 1–35.

Wiszniewska J., Krzemińska E., 2021. Advances in geochronology in the Suwałki anorthosite massif and subsequent granite veins, northeastern Poland. Precambrian Research, **361**, 106265; https://doi.org/10.1016/j.precamres.2021.106265

Vermeesch, P., 2012. On the visualisation of detrital age distributions. Chemical Geology, **312:** 190–194; https://doi.org/10.1016/j.chemgeo.2012.04.021

Vermeesch, P., 2013. Multi-sample comparison of detrital age distributions. Chemical Geology, **341**: 140–146; https://doi.org/10.1016/j.chemgeo.2013.01.010

Vermeesch, P., 2018. IsoplotR: a free and open toolbox for geochronology. Geoscience Frontiers, **9**: 1479–1493; https://doi.org/10.1016/j.gsf.2018.04.001

Zaitseva, T.S., Kuzmenkova, O.F., Kuznetsov, A.B., Kovach, V.P., Gorokhovsky, B.M., Plotkina, Yu.V., Adamskaya, E.V., Laptsevich, A.G., 2023. The U-Th-Pb Age of detrital zircon from the Riphean sandstones of the Volyn-Orsha Paleotrough. Stratigraphy and Geological Correlation, **31**: 390–409; https://doi.org/10.31857/S0869592X23050101

Zametzer, A., Dröllner, M., Barham, M., Kirkland, C.L., Norris, A., 2025. Grain selection for representative detrital zircon age populations, Earth and Planetary Science Letters, **671**, 119619; https://doi.org/10.1016/j.epsl.2025.119619

Żelaźniewicz, A., Oberc-Dziedzic, T., Slama, J., 2020. Baltica and the Cadomian orogen in the Ediacaran–Cambrian: a perspective from SE Poland. International Journal of Earth Science, **109**: 1503–1528; https://doi.org/10.1007/s00531-020-01858-0

Żelichowski, A.M., 1972. Geological setting of the area between Holy Cross Mountains and Bug river (in Polish with English summary). Biuletyn Instytutu Geologicznego, **263**: 1–97.

Supplementary Table 1. The U-Pb SHRIMP analytical data for zircon grains from Kaplonosy IG 1 subsamples Kap-1875.5j and Kap-1875.5c

Kaplonosy IG 1 depth 1875.5m sample Kap-1875.5 c

youngest zircon age

Spot	$^{204}Pb/^{206}Pb$	±%	$^{207}Pb/^{206}Pb$	±%	$^{208}Pb/^{206}Pb$	±%	$^{206}Pb/^{238}U$	±%	$^{206}Pb_c$ [%]	U [ppm]	Th [ppm]	4-corr ppm $^{206}Pb^*$	4-corr ppm $^{208}Pb^*$	$^{232}Th/^{238}U$	±%	(1) $^{206}Pb/^{238}U$ Age		(2) $^{206}Pb/^{238}U$ Age		(3) $^{206}Pb/^{238}U$ Age		(1) $^{207}Pb/^{206}Pb$ Age		% Discordant	7-corr $^{208}Pb^*/^{232}Th$	±%	(1) $^{238}U/^{206}Pb^*$	±%	(1) $^{207}Pb^*/^{206}Pb^*$	±%	(1) $^{207}Pb^*/^{235}U$	±%	(1) $^{206}Pb^*/^{238}U$	±%	err corr
Kap_1875c.4.1	8.6E-5	58	0.076	1.2	0.192	0.79	0.41	1.0	0.156	77	38	11.6	2.2	0.52	0.30	1044	18	1043	18	1027	19	1067	31	+2	0.064	2.6	5.69	1.8	0.075	1.5	1.8	2.4	0.176	1.8	0.76
Kap_1875c.8.1	–	–	0.089	0.9	0.129	0.73	0.65	0.4	0.000	76	25	15.2	2.0	0.33	0.29	1358	24	1354	26	1339	25	1407	16	+4	0.086	3.8	4.27	2.0	0.089	0.9	2.9	2.2	0.234	2.0	0.92
Kap_1875c.9.1	–	–	0.095	0.8	0.373	1.30	0.68	1.3	0.000	75	73	16.3	6.1	1.01	0.59	1451	23	1444	25	1397	28	1531	15	+6	0.091	2.5	3.96	1.8	0.095	0.8	3.3	2.0	0.253	1.8	0.92
Kap_1875c.5.1	2.5E-5	100	0.092	1.0	0.400	0.55	0.44	1.3	0.045	87	94	19.6	7.9	1.11	0.30	1493	26	1496	29	1440	32	1458	21	-3	0.095	2.4	3.84	2.0	0.092	1.1	3.3	2.2	0.261	2.0	0.88
Kap_1875c.3.1	1.1E-4	58	0.095	1.2	0.328	1.36	0.68	1.8	0.203	39	32	8.7	2.8	0.86	0.50	1497	26	1498	28	1445	30	1494	30	-0	0.099	2.9	3.82	1.9	0.093	1.6	3.4	2.5	0.261	1.9	0.77
Kap_1875c.11.1	-4E-5	100	0.097	2.1	0.426	0.69	0.72	1.1	-0.072	36	38	8.1	3.5	1.09	0.47	1500	26	1492	28	1421	31	1583	41	+6	0.100	2.7	3.82	1.9	0.098	2.2	3.5	2.9	0.262	1.9	0.66
Kap_1875c.1.1	-4E-5	71	0.093	0.8	0.540	0.42	0.64	1.8	-0.063	87	124	19.8	10.8	1.46	0.30	1514	26	1516	29	1426	34	1498	17	-1	0.098	2.2	3.78	1.9	0.094	0.9	3.4	2.2	0.265	1.9	0.91
Kap_1875c.2.1	-2E-5	100	0.103	0.8	0.123	1.86	0.77	1.6	-0.030	65	20	15.8	2.0	0.32	1.58	1603	26	1594	28	1581	27	1682	15	+5	0.098	5.3	3.54	1.8	0.103	0.8	4.0	2.0	0.282	1.8	0.91
Kap_1875c.6.1	-3E-5	71	0.110	0.7	0.234	0.49	0.79	1.7	-0.047	74	46	19.6	4.7	0.64	0.28	1727	27	1717	31	1687	30	1799	13	+5	0.107	3.1	3.26	1.8	0.110	0.7	4.7	1.9	0.307	1.8	0.93
Kap_1875c.7.1	4.4E-5	100	0.109	1.2	0.292	0.83	0.85	1.7	0.079	32	25	8.9	2.6	0.78	0.53	1796	31	1798	36	1743	35	1776	25	-1	0.121	3.4	3.11	2.0	0.109	1.4	4.8	2.4	0.321	2.0	0.82
Kap_1875c.10.1	1.7E-5	71	0.122	0.8	0.155	0.48	0.72	1.3	0.031	149	64	45.7	7.1	0.44	0.22	1971	30	1969	36	1947	32	1981	15	+1	0.123	5.4	2.80	1.8	0.122	0.9	6.0	2.0	0.358	1.8	0.90
Kap_1875c.30.1	-6.4E-5	100	0.0763	1.78	0.128	1.42	0.35	1.5	–	39	16	5.5	0.7	0.41	0.92	986	±18	980	±18	984	±19	1126	±42	+13	0.0465	4.3	6.05	1.9	0.0772	2.11	1.76	2.9	0.165	1.9	0.68
Kap_1875c.42.1	4.8E-5	58	0.0920	0.82	0.545	1.97	0.66	1.0	0.08	64	118	10.0	5.5	1.90	1.11	1076	±16	1057	±17	1093	±23	1454	±18	+28	0.0480	2.8	5.50	1.6	0.0914	0.93	2.29	1.9	0.182	1.6	0.87
Kap_1875c.27.1	-2.8E-5	100	0.0751	1.18	0.186	0.79	0.48	1.4	–	70	41	11.6	2.2	0.61	0.33	1146	±16	1149	±17	1143	±17	1082	±26	-6	0.0622	2.3	5.14	1.5	0.0755	1.29	2.03	2.0	0.195	1.5	0.76
Kap_1875c.34.1	-9.3E-5	50	0.0769	1.08	0.115	0.91	0.47	2.0	–	76	28	12.9	1.5	0.38	1.04	1158	±24	1158	±26	1156	±26	1152	±27	-1	0.0611	3.9	5.08	2.3	0.0782	1.36	2.12	2.7	0.197	2.3	0.86
Kap_1875c.48.1	-2.5E-4	30	0.0765	1.14	0.145	0.87	0.51	3.9	–	67	32	11.4	1.8	0.50	0.57	1167	±10	1165	±11	1165	±11	1197	±34	+3	0.0597	2.2	5.04	1.0	0.0800	1.71	2.19	2.0	0.198	1.0	0.49
Kap_1875c.45.1	-1.3E-4	50	0.0803	1.24	0.186	0.86	0.59	0.8	–	35	22	6.3	1.2	0.63	0.71	1218	±20	1216	±21	1216	±21	1250	±32	+3	0.0620	2.8	4.81	1.8	0.0822	1.65	2.36	2.4	0.208	1.8	0.73
Kap_1875c.54.1	-6.0E-5	50	0.0801	0.83	0.184	0.58	0.54	1.2	–	74	44	13.4	2.5	0.61	0.47	1223	±14	1223	±15	1220	±15	1219	±19	-0	0.0642	2.0	4.79	1.3	0.0809	0.98	2.33	1.6	0.209	1.3	0.79
Kap_1875c.39.1	2.6E-4	38	0.0924	1.27	0.354	4.08	0.45	5.5	0.42	58	57	12.4	4.3	1.01	1.47	1435	±13	1438	±14	1404	±19	1400	±39	-3	0.0862	4.6	4.01	1.0	0.0888	2.03	3.05	2.3	0.249	1.0	0.46
Kap_1875c.50.1	1.1E-4	38	0.0929	1.54	0.417	1.45	0.69	1.2	0.19	53	71	11.4	4.7	1.39	2.26	1439	±18	1438	±20	1435	±24	1453	±32	+1	0.0743	3.2	4.00	1.4	0.0913	1.70	3.15	2.2	0.250	1.4	0.64
Kap_1875c.20.1	1.1E-4	41	0.0942	0.86	0.117	0.79	0.63	1.1	0.18	56	21	12.2	1.4	0.39	0.66	1450	±19	1448	±21	1451	±20	1480	±21	+2	0.0709	3.6	3.96	1.5	0.0926	1.12	3.22	1.9	0.252	1.5	0.80
Kap_1875c.17.1	–	–	0.0919	1.29	0.492	2.26	0.63	0.5	–	31	56	6.9	3.4	1.85	0.65	1473	±26	1473	±28	1512	±35	1466	±24	-1	0.0685	3.2	3.90	2.0	0.0919	1.29	3.25	2.4	0.257	2.0	0.84
Kap_1875c.24.1	–	–	0.0950	1.90	0.553	0.92	0.72	1.4	0.00	33	59	7.3	4.1	1.85	0.34	1483	±25	1479	±27	1475	±33	1529	±36	+3	0.0766	2.4	3.87	1.9	0.0950	1.90	3.39	2.7	0.259	1.9	0.70
Kap_1875c.41.1	–	–	0.0943	0.80	0.319	2.05	0.70	2.0	–	61	61	13.6	4.4	1.03	1.49	1484	±12	1481	±13	1474	±15	1515	±15	+2	0.0789	2.8	3.86	0.9	0.0943	0.80	3.37	1.2	0.259	0.9	0.75
Kap_1875c.46.1	1.5E-5	58	0.0912	0.46	0.133	0.39	0.69	1.1	0.03	179	85	39.9	5.3	0.49	0.32	1486	±13	1489	±14	1493	±14	1446	±9	-3	0.0729	1.9	3.86	1.0	0.0910	0.48	3.25	1.1	0.259	1.0	0.90
Kap_1875c.49.1	5.3E-5	50	0.0926	0.73	0.131	0.63	0.70	1.0	0.09	69	30	15.4	2.0	0.44	0.54	1486	±18	1488	±19	1486	±19	1465	±16	-2	0.0778	2.8	3.86	1.3	0.0919	0.84	3.28	1.6	0.259	1.3	0.85
Kap_1875c.43.1	1.3E-4	38	0.0934	0.87	0.428	0.47	0.66	1.3	0.21	51	74	11.4	4.9	1.50	0.96	1494	±32	1497	±35	1506	±41	1459	±22	-3	0.0747	2.9	3.83	2.4	0.0916	1.17	3.29	2.7	0.261	2.4	0.90
Kap_1875c.16.1	-3.4E-5	58	0.0946	0.67	0.210	0.47	0.68	1.1	–	95	65	21.4	4.6	0.70	0.90	1496	±17	1493	±18	1493	±18	1530	±14	+2	0.0768	2.1	3.83	1.2	0.0951	0.72	3.43	1.4	0.261	1.2	0.87
Kap_1875c.59.1	2.3E-5	71	0.0933	0.69	0.334	0.41	0.66	2.9	0.04	79	87	17.8	6.0	1.13	0.40	1503	±17	1505	±18	1504	±20	1488	±14	-1	0.0776	1.6	3.81	1.2	0.0930	0.73	3.37	1.4	0.263	1.2	0.86
Kap_1875c.44.1	4.7E-5	50	0.0947	0.68	0.407	1.40	0.51	0.7	0.08	116	164	26.6	10.9	1.46	0.83	1520	±16	1521	±17	1537	±20	1510	±14	-1	0.0743	2.1	3.76	1.2	0.0941	0.76	3.45	1.4	0.266	1.2	0.84
Kap_1875c.60.1	3.6E-5	71	0.0942	0.84	0.266	0.55	0.66	1.1	0.06	55	46	12.5	3.3	0.88	0.53	1522	±20	1524	±22	1518	±23	1503	±17	-1	0.0812	2.1	3.75	1.5	0.0937	0.93	3.44	1.7	0.266	1.5	0.85
Kap_1875c.40.1	2.9E-5	100	0.0935	1.10	0.483	6.40	0.66	2.2	0.05	33	46	7.6	3.7	1.43	9.61	1525	±24	1528	±27	1479	±52	1490	±22	-3	0.0908	11.7	3.75	1.8	0.0931	1.19	3.43	2.2	0.267	1.8	0.84
Kap_1875c.63.1	1.4E-4	38	0.0965	0.87	0.291	0.55	0.49	1.9	0.22	68	67	15.6	4.5	1.01	0.50	1526	±19	1527	±21	1533	±22	1521	±22	-0	0.0762	2.0	3.74	1.4	0.0946	1.18	3.48	1.8	0.267	1.4	0.77
Kap_1875c.38.1	4.5E-5	58	0.0944	0.77	0.326	0.46	0.66	0.9	0.07	66	69	15.5	5.1	1.09	0.47	1563	±19	1569	±21	1559	±22	1503	±16	-5	0.0842	1.8	3.64	1.4	0.0938	0.87	3.55	1.6	0.274	1.4	0.84
Kap_1875c.61.1	-4.5E-6	100	0.1104	0.39	0.171	0.36	0.69	1.2	–	200	109	47.4	8.2	0.56	0.31	1572	±21	1549	±23	1568	±23	1807	±7	+15	0.0658	2.9	3.62	1.5	0.1104	0.40	4.21	1.6	0.276	1.5	0.97
Kap_1875c.37.1	-6.3E-5	38	0.0935	0.60	0.285	0.99	0.66	2.2	–	100	89	23.8	6.9	0.92	0.38	1576	±16	1582	±18	1565	±18	1515	±13	-5	0.0886	1.8	3.61	1.2	0.0943	0.69	3.60	1.3	0.277	1.2	0.86
Kap_1875c.56.1	-2.6E-4	33	0.0945	1.07	0.757	0.54	0.64	1.2	–	43	103	10.5	8.1	2.50	2.38	1628	±25	1632	±27	1597	±41	1587	±30	-3	0.0884	3.0	3.48	1.7	0.0980	1.59	3.88	2.3	0.287	1.7	0.73
Kap_1875c.19.1	3.7E-5	38	0.1094	0.48	0.145	0.38	0.67	1.6	0.06	193	105	48.8	7.1	0.56	0.94	1661	±15	1648	±16	1676	±16	1781	±9	+8	0.0646	2.6	3.40	1.0	0.1089	0.51	4.41	1.1	0.294	1.0	0.89
Kap_1875c.28.1	-3.5E-5	41	0.1104	0.50	0.183	0.59	0.62	1.2	–	172	107	44.0	8.2	0.64	0.32	1681	±29	1667	±32	1684	±32	1814	±10	+8	0.0749	3.6	3.36	2.0	0.1109	0.53	4.56	2.0	0.298	2.0	0.97
Kap_1875c.15.1	1.4E-5	100	0.1101	0.70	0.274	0.48	0.83	0.8	0.02	65	61	16.9	4.7	0.96	0.50	1700	±22	1689	±24	1704	±25	1798	±13	+6	0.0806	2.3	3.32	1.5	0.1099	0.72	4.57	1.6	0.302	1.5	0.90
Kap_1875c.36.1	1.8E-5	71	0.1078	0.60	0.358	3.84	0.82	3.3	0.03	110	156	28.6	10.3	1.46	0.36	1702	±52	1695	±58	1756	±64	1758	±11	+4	0.0718	5.8	3.31	3.5	0.1076	0.62	4.48	3.6	0.302	3.5	0.98
Kap_1875c.51.1	5.5E-5	40	0.1105	0.55	0.229	0.40	0.52	1.6	0.09	170	130	44.2	10.2	0.79	0.37	1706	±12	1696	±14	1708	±14	1795	±11	+6	0.0815	1.6	3.30	0.8	0.1097	0.61	4.58	1.0	0.303	0.8	0.80
Kap_1875c.57.1	-4.0E-5	58	0.1085	0.68	0.250	2.69	0.77	2.5	–	57	41	15.1	3.8	0.74	2.12	1720	±21	1713	±24	1694	±24	1783	±13	+4	0.0990	4.1	3.27	1.4	0.1090	0.73	4.60	1.6	0.306	1.4	0.89
Kap_1875c.18.1	1.7E-5	71	0.1091	0.54	0.122	0.52	0.56	1.6	0.03	137	56	36.5	4.5	0.42	0.44	1742	±13	1737	±14	1742	±13	1780	±10	+2	0.0845	2.6	3.22	0.8	0.1088	0.56	4.66	1.0	0.310	0.8	0.83
Kap_1875c.12.1	2.1E-4	38	0.1136	1.01	0.114	1.02	0.45	1.1	0.33	74	28	19.9	2.2	0.39	0.81	1750	±26	1743	±29	1754	±28	1812	±26	+4	0.0771	6.1	3.21	1.7	0.1108	1.43	4.76	2.2	0.312	1.7	0.77
Kap_1875c.29.1	-2.8E-5	71	0.1120	0.69	0.304	0.46	0.57	1.6	–	96	98	25.8	7.9	1.06	1.15	1759	±20	1749	±22	1760	±23	1838	±13	+5	0.0863	2.3	3.19	1.3	0.1124	0.73	4.86	1.5	0.314	1.3	0.87
Kap_1875c.13.1	–	–	0.1071	0.53	0.158	0.46	0.82	1.0	0.00	107	58	29.0	4.6	0.56	1.34	1773	±18	1776	±21	1776	±20	1751	±10	-1	0.0919	2.9	3.16	1.2	0.1071	0.53	4.68	1.3	0.317	1.2	0.91
Kap_1875c.26.1	4.0E-5	58	0.1108	0.69	0.314	1.55	0.83	1.5	0.06	66	69	17.9	5.6	1.08	0.27	1776	±22	1772	±25	1776	±26	1804	±14	+2	0.0904	2.6	3.15	1.4	0.1103	0.75	4.82	1.6	0.317	1.4	0.89
Kap_1875c.22.1	1.2E-4	41	0.1119	0.82	0.160	1.82	0.55	1.1	0.18	72	39	19.5	3.1	0.57	2.16	1778	±23	1774	±26	1783	±25	1805	±19	+2	0.0853	4.5	3.15	1.5	0.1103	1.02	4.83	1.8	0.318	1.5	0.82
Kap_1875c.52.1	1.1E-4	27	0.1098	0.53	0.180	0.48	0.77	3.4	0.17	100	61	27.3	4.9	0.64	0.39	1785	±18	1787	±20	1792	±20	1772	±12	-1	0.0893	2.4	3.13	1.2	0.1083	0.65	4.77	1.3	0.319	1.2	0.87
Kap_1875c.53.1	9.6E-6	100	0.1103	0.57	0.139	0.52	0.91	1.4	0.01	78	37	21.7	3.1	0.49	0.50	1802	±20	1802	±23	1803	±22	1803	±11	+0	0.0922	3.3	3.10	1.3	0.1102	0.59	4.90	1.4	0.322	1.3	0.91
Kap_1875c.47.1	7.5E-5	45	0.1116	0.71	0.285	0.94	0.86	1.7	0.12	52	51	14.5	4.2	1.02	0.24	1807	±24	1807	±27	1815	±27	1809	±15	+0	0.0900	2.5	3.09	1.5	0.1106	0.83	4.93	1.7	0.323	1.5	0.88
Kap_1875c.21.1	-6.7E-5	58	0.1099	0.88	0.618	1.33	0.79	1.7	–	42	84	11.8	7.4	2.06	0.58	1816	±27	1816	±30	1793	±38	1812	±18	-0	0.0979	2.4	3.07	1.7	0.1108	0.99	4.97	2.0	0.325	1.7	0.86
Kap_1875c.23.1	-1.2E-5	71	0.1111	0.44	0.283	0.80	0.89	1.2	–	136	128	38.1	10.9	0.97	0.32	1824	±28	1824	±31	1822	±32	1820	±8	-0	0.0954	2.7	3.06	1.8	0.1112	0.45	5.02	1.8	0.327	1.8	0.97
Kap_1875c.35.1	–	–	0.1095	0.43	0.274	0.30	0.84	1.5	–	166	150	46.8	12.9	0.93	0.32	1826	±17	1831	±19	1823	±19	1791	±8	-2	0.0984	1.7	3.05	1.1	0.1095	0.43	4.94	1.2	0.328	1.1	0.93
Kap_1875c.31.1	2.8E-5	58	0.1104	0.56	0.165	0.48	0.88	0.6	0.04	88	49	24.9	4.1	0.57	0.47	1829	±20	1833	±23	1829	±22	1799	±11	-2	0.0983	2.8	3.05	1.3	0.1100	0.60	4.98	1.4	0.328	1.3	0.90
Kap_1875c.55.1	-4.3E-4	26	0.1103	1.00	0.181	0.81	0.88	1.4	--	33	20	9.4	1.8	0.62	0.81	1830	±49	1822	±55	1818	±52	1896	±29	+4	0.0967	6.1	3.05	3.1	0.1160	1.59	5.25	3.4	0.328	3.1	0.89
Kap_1875c.32.1	3.1E-5	50	0.1114	0.52	0.249	0.37	0.76	2.4	0.05	124	101	35.2	8.8	0.84	0.39	1844	±18	1848	±21	1839	±21	1815	±10	-2	0.0999	2.0	3.02	1.2	0.1110	0.55	5.07	1.3	0.331	1.2	0.90
Kap_1875c.25.1	1.4E-5	71	0.1094	0.50	0.226	0.37	0.84	1.5	0.02	121	91	34.8	7.9	0.77	0.17	1853	±18	1862	±21	1850	±20	1786	±9	-4	0.1027	2.0	3.00	1.1	0.1092	0.51	5.02	1.3	0.333	1.1	0.91
Kap_1875c.14.1	-4.1E-4	27	0.1085	1.03	0.341	0.64	0.48	1.7	–	64	74	18.4	6.6	1.19	0.63	1857	±27	1856	±31	1849	±32	1865	±29	+0	0.0987	2.6	2.99	1.7	0.1141	1.62	5.25	2.4	0.334	1.7	0.72
Kap_1875c.62.1	-1.6E-5	100	0.1090	0.75	0.253	0.90	0.41	1.2	–	150	130	43.1	11.0	0.90	0.47	1860	±21	1870	±24	1864	±24	1786	±14	-5	0.0996	2.4	2.99	1.3	0.1092	0.78	5.04	1.5	0.335	1.3	0.86
Kap_1875c.58.1	8.3E-6	100	0.1130	0.53	0.120	1.53	0.83	1.2	0.01	106	59	30.6	3.7	0.58	4.65	1872	±20	1875	±22	1908	±22	1846	±10	-2	0.0724	6.0	2.97	1.2	0.1129	0.54	5.24	1.3	0.337	1.2	0.91
Kap_1875c.33.1	4.8E-5	58	0.1136	0.75	0.208	0.59	0.88	2.0	0.07	52	36	15.3	3.2	0.72	1.35	1902	±56	1910	±65	1903	±62	1847	±15	-3	0.1033	6.5	2.91	3.4	0.1130	0.82	5.35	3.5	0.343	3.4	0.97
Kap_1875c.64.1	–	–	0.095	0.64	0.130	0.56	0.73	1.5	-6E-10	128	47	32	4.2	0.4	0.92	1632	27.0	1644	30	1618	28	1525	12.1	-8	0.1120	4.0	3.471	1.9	0.095	0.64	3.768	2.0	0.288	1.9	0.95
Kap_1875c.65.1	2.5E-5	71	0.094	0.72	0.275	1.61	0.68	1.8	0.04	117.18	84.28	26.88	7.4	0.74	0.95	1526	25.6	1528	28	1486	29.0	1496	14.6	-2	0.1000	3.1	3.745	1.9	0.093	0.77	3.438	2.0	0.267	1.9	0.93
Kap_1875c.66.1	2.6E-5	71	0.094	0.72	0.182	0.54	0.80	1.2	0.05	113.44	52.50	25.66	4.7	0.48	0.27	1507	32.1	1508	35	1479	34.5	1494	14.6	-1	0.1007	3.8	3.797	2.4	0.093	0.77	3.388	2.5	0.263	2.4	0.95
Kap_1875c.67.1	7.7E-5	45	0.076	0.87	0.153	0.72	0.45	2.1	0.14	156.11	61.32	24.61	3.7	0.41	1.06	1086	24.1	1088	25	1072	25.7	1059	22.3	-3	0.0691	3.4	5.449	2.4	0.075	1.11	1.889	2.7	0.184	2.4	0.91
Kap_1875c.68.1	-2.0E-5	45	0.112	0.38	0.312	0.52	0.79	1.6	-0.04	299.53	248.75	83.92	26.5	0.86	0.16	1820	29.9	1817	34	1764	34.2	1837	7.1	1	0.1177	2.8	3.066	1.9	0.112	0.39	5.050	1.9	0.326	1.9	0.98
Kap_1875c.69.1	-3.6E-5	100	0.096	1.22	0.238	2.82	0.65	4.3	-0.06	54.52	36.62	11.76	2.8	0.69	2.06	1444	24.6	1434	27	1421	27.9	1556	24.6	8	0.0805	4.5	3.983	1.9	0.096	1.31	3.338	2.3	0.251	1.9	0.82
Kap_1875c.70.1	-5.2E-5	50	0.093	0.72	0.651	0.34	0.72	1.8	-0.09	95.69	158.35	21.67	14.3	1.71	0.64	1509	26.8	1508	29	1383	37.0	1512	15.3	0	0.1006	2.2	3.793	2.0	0.094	0.81	3.425	2.1	0.264	2.0	0.93
Kap_1875c.71.1	5.2E-5	100	0.096	1.45	0.543	2.57	0.65	2.2	0.09	31.06	44.25	7.32	4.0	1.47	1.40	1564	27.6	1567	31	1473	38.1	1530	31.0	-2	0.1020	3.7	3.643	2.0	0.095	1.65	3.599	2.6	0.275	2.0	0.77
Kap_1875c.72.1	-1.5E-5	100	0.095	0.78	0.323	1.87	0.74	0.9	-0.03	89.52	73.92	20.68	6.8	0.85	1.11	1536	24.6	1536	27	1481	28.7	1526	15.3	-1	0.1026	3.1	3.718	1.8	0.095	0.81	3.520	2.0	0.269	1.8	0.91
Kap_1875c.73.1	-6.5E-5	58	0.074	1.03	0.128	0.82	0.48	1.9	-0.12	110.21	35.65	18.36	2.4	0.33	0.28	1143	20.4	1146	22	1127	21.4	1078	24.9	-7	0.0795	3.1	5.156	1.9	0.075	1.24	2.015	2.3	0.194	1.9	0.84
Kap_1875c.74.1	-8.2E-5	100	0.093	1.81	0.454	0.96	0.71	0.8	-0.15	20.75	24.55	4.71	2.2	1.22	0.66	1511	28.4	1510	31	1437	35.0	1521	40.6	1	0.0982	2.8	3.786	2.1	0.095	2.15	3.446	3.0	0.264	2.1	0.70
Kap_1875c.75.1	4.9E-5	41	0.108	0.53	0.211	1.69	0.71	1.4	0.09	162.55	101.55	34.45	7.3	0.65	1.13	1422	25.9	1391	27	1409	28.6	1753	10.9	21	0.0604	3.8	4.053	2.0	0.107	0.59	3.647	2.1	0.247	2.0	0.96
Kap_1875c.76.1	-2.6E-5	71	0.110	1.08	0.208	0.51	0.80	1.4	-0.05	93.99	51.78	25.85	5.4	0.57	0.28	1790	30.7	1789	35	1755	33.4	1798	20.1	1	0.1165	4.0	3.124	2.0	0.110	1.10	4.853	2.3	0.320	2.0	0.87
Kap_1875c.77.1	1.2E-4	50	0.111	1.03	0.248	0.74	0.73	2.3	0.22	60.82	41.04	15.02	3.7	0.70	0.41	1628	34.5	1610	38	1598	38.5	1786	23.5	10	0.0894	4.0	3.480	2.4	0.109	1.29	4.327	2.7	0.287	2.4	0.88
Kap_1875c.78.1	-2.7E-4	35	0.110	1.08	0.216	0.82	0.52	1.6	-0.49	72.05	42.67	19.03	4.3	0.61	0.62	1728	34.8	1709	39	1691	37.9	1867	27.8	8	0.1002	4.4	3.253	2.3	0.114	1.54	4.840	2.8	0.307	2.3	0.83
Kap_1875c.79.1	-3.3E-5	50	0.112	0.53	0.252	0.83	0.78	2.3	-0.06	161.73	120.62	44.34	11.3	0.77	0.76	1786	31.1	1777	35	1761	34.9	1846	10.2	4	0.0998	3.4	3.133	2.0	0.113	0.56	4.966	2.1	0.319	2.0	0.96
Kap_1875c.80.1	-5.1E-5	33	0.111	0.44	0.152	0.63	0.71	1.5	-0.09	251.07	101.61	68.50	10.6	0.42	0.18	1778	27.2	1772	31	1753	28.9	1820	8.7	3	0.1105	4.1	3.148	1.8	0.111	0.48	4.872	1.8	0.318	1.8	0.96
Kap_1875c.81.1	-3.1E-5	71	0.109	1.15	0.282	0.49	0.89	1.0	-0.06	72.66	54.13	20.05	5.7	0.77	0.32	1795	28.5	1797	33	1745	32.1	1787	21.5	-1	0.1189	3.1	3.114	1.8	0.109	1.18	4.837	2.2	0.321	1.8	0.84
Kap_1875c.82.1	7.8E-5	32	0.112	0.51	0.183	0.42	0.75	2.2	0.14	152.05	88.32	41.23	7.5	0.60	0.21	1769	27.3	1761	31	1763	29.7	1822	10.9	3	0.0896	3.7	3.168	1.8	0.111	0.60	4.847	1.9	0.316	1.8	0.95

Errors are 1-sigma; Pb_c and Pb^* indicate the common and radiogenic portions. respectively.

Error in Standard calibration was 0.30% (not included in above errors but required when comparing data from different mounts).

(1) Common Pb corrected using measured ^{204}Pb.

(2) Common Pb corrected by assuming $^{206}Pb/^{238}U$-$^{207}Pb/^{235}U$ age-concordance

(3) Common Pb corrected by assuming $^{206}Pb/^{238}U$-$^{208}Pb/^{232}Th$ age-concordance

Kaplonosy IG 1 depth 1875.5m sample Kap-1875.5 j

youngest zircon age

Spot	$^{204}Pb/^{206}Pb$	±%	$^{207}Pb/^{206}Pb$	±%	$^{208}Pb/^{206}Pb$	±%	$^{206}Pb/^{238}U$	±%	$^{206}Pb_c$ [%]	U [ppm]	Th [ppm]	4-corr ppm $^{206}Pb^*$	4-corr ppm $^{208}Pb^*$	$^{232}Th/^{238}U$	±%	(1) $^{206}Pb/^{238}U$ Age		(2) $^{206}Pb/^{238}U$ Age		(3) $^{206}Pb/^{238}U$ Age		(1) $^{207}Pb/^{206}Pb$ Age		% Discordant	7corr $^{208}Pb^*/^{232}Th$	±%	(1) $^{238}U/^{206}Pb^*$	±%	(1) $^{207}Pb^*/^{206}Pb^*$	±%	(1) $^{207}Pb^*/^{235}U$	±%	(1) $^{206}Pb^*/^{238}U$	±%	err corr
Kap_1875j.8.1	4.9E-5	71	0.082	1.06	0.12	0.91	0.33	2.5	0.09	103	33	15.1	1.8	0.33	0.26	1016	±14	1006	±14	1008	±15	1230	±24	+19	0.048	3.4	5.86	1.5	0.081	1.23	1.91	1.9	0.171	1.5	0.77
Kap_1875j.35.1	–		0.080	1.92	0.35	1.04	0.55	1.4	0.00	21	18	3.3	1.2	0.88	0.56	1060	±17	1053	±18	1017	±20	1191	±38	+12	0.067	2.5	5.60	1.7	0.080	1.92	1.97	2.6	0.179	1.7	0.67
Kap_1875j.42.1	2.1E-4	35	0.078	1.12	0.11	0.98	0.34	1.3	0.38	84	24	13.2	1.3	0.29	0.75	1078	±15	1078	±15	1072	±15	1080	±37	+0	0.063	3.5	5.49	1.5	0.075	1.83	1.89	2.4	0.182	1.5	0.63
Kap_1875j.31.1	–		0.078	1.14	0.15	0.86	0.49	0.8	0.00	73	28	12.1	1.8	0.40	0.32	1144	±16	1145	±17	1129	±17	1137	±23	-1	0.073	2.7	5.15	1.5	0.078	1.14	2.08	1.9	0.194	1.5	0.80
Kap_1875j.10.1	-2.9E-4	33	0.078	1.22	0.36	1.10	0.39	1.6	–	77	72	13.0	4.8	0.96	0.32	1157	±19	1151	±20	1112	±23	1254	±39	+8	0.072	2.4	5.09	1.8	0.082	1.99	2.23	2.7	0.197	1.8	0.68
Kap_1875j.5.1	8.2E-5	58	0.090	1.06	0.14	0.88	0.36	1.8	0.15	92	53	16.4	2.3	0.59	0.29	1209	±20	1197	±21	1230	±21	1402	±25	+15	0.041	3.6	4.85	1.8	0.089	1.31	2.53	2.2	0.206	1.8	0.80
Kap_1875j.23.1	9.5E-5	32	0.081	0.66	0.12	1.67	0.44	1.1	0.17	167	51	29.8	3.4	0.31	1.33	1219	±17	1221	±18	1208	±18	1181	±17	-4	0.078	3.4	4.81	1.5	0.079	0.86	2.28	1.8	0.208	1.5	0.87
Kap_1875j.18.1	-1.9E-5	71	0.083	0.64	0.16	0.76	0.56	0.9	–	164	66	30.7	4.9	0.41	0.20	1271	±18	1270	±20	1251	±20	1286	±13	+1	0.082	2.5	4.59	1.6	0.084	0.68	2.52	1.7	0.218	1.6	0.92
Kap_1875j.9.1	–		0.083	0.73	0.12	0.63	0.60	1.9	–	109	33	20.6	2.5	0.31	0.23	1284	±17	1285	±18	1268	±18	1268	±14	-1	0.085	2.8	4.54	1.5	0.083	0.73	2.52	1.6	0.220	1.5	0.89
Kap_1875j.11.1	2.9E-4	41	0.092	1.41	0.22	0.97	0.44	1.7	0.52	45	26	8.5	1.8	0.60	0.42	1285	±19	1278	±20	1267	±20	1379	±46	+8	0.072	2.9	4.53	1.6	0.088	2.41	2.67	2.9	0.221	1.6	0.55
Kap_1875j.14.1	4.0E-5	58	0.113	1.06	0.18	1.02	0.37	1.6	0.07	179	88	36.1	6.4	0.51	0.21	1360	±18	1317	±19	1345	±19	1839	±20	+29	0.047	4.5	4.26	1.4	0.112	1.10	3.64	1.8	0.235	1.4	0.80
Kap_1875j.48.1	-2.1E-5	50	0.106	0.44	0.15	1.13	0.69	3.4	–	184	61	38.7	5.9	0.35	0.27	1414	±18	1384	±19	1383	±19	1738	±8	+21	0.072	3.3	4.08	1.4	0.106	0.45	3.60	1.5	0.245	1.4	0.95
Kap_1875j.13.1	-1.3E-4	100	0.093	2.29	0.38	1.28	0.39	1.9	–	18	19	3.9	1.5	1.06	0.65	1431	±24	1424	±26	1382	±29	1514	±55	+6	0.087	3.0	4.02	1.9	0.094	2.92	3.23	3.5	0.249	1.9	0.54
Kap_1875j.49.1	2.1E-4	50	0.095	1.52	0.53	3.19	0.58	1.5	0.38	25	34	5.4	2.8	1.41	2.76	1449	±22	1447	±24	1366	±33	1472	±43	+2	0.093	4.6	3.97	1.7	0.092	2.25	3.21	2.8	0.252	1.7	0.60
Kap_1875j.6.1	-8.7E-5	50	0.093	0.94	0.69	1.44	0.69	0.9	–	49	88	10.6	7.4	1.85	1.26	1451	±20	1446	±22	1333	±30	1509	±21	+4	0.093	2.5	3.96	1.5	0.094	1.13	3.27	1.9	0.253	1.5	0.80
Kap_1875j.17.1	1.8E-5	100	0.096	0.83	0.60	0.40	0.65	0.4	0.03	64	101	14.0	8.4	1.63	0.30	1461	±20	1453	±21	1367	±26	1548	±16	+6	0.091	1.7	3.93	1.5	0.096	0.87	3.37	1.7	0.254	1.5	0.86
Kap_1875j.43.1	1.8E-4	28	0.094	1.26	0.41	1.56	0.47	1.3	0.32	136	148	29.8	12.2	1.13	1.51	1463	±19	1464	±21	1408	±24	1449	±29	-1	0.092	2.8	3.93	1.5	0.091	1.51	3.20	2.1	0.255	1.5	0.70
Kap_1875j.47.1	-1.3E-5	100	0.094	0.73	0.27	1.49	0.53	1.4	–	99	70	21.8	5.9	0.73	1.11	1472	±19	1469	±21	1435	±22	1512	±14	+3	0.093	2.7	3.90	1.5	0.094	0.75	3.33	1.6	0.257	1.5	0.89
Kap_1875j.26.1	-3.8E-4	50	0.095	1.95	0.43	1.05	0.59	0.8	–	13	15	2.9	1.3	1.16	0.66	1474	±25	1458	±27	1396	±30	1633	±59	+11	0.093	2.7	3.89	1.9	0.100	3.15	3.56	3.7	0.257	1.9	0.51

Kap_1875j.28.1	–		0.095	0.64	0.20	1.87	0.73	2.2	–	84	43	18.5	3.7	0.53	1.49	1476	±19	1471	±21	1447	±21	1533	±12	+4	0.093	3.3	3.89	1.5	0.095	0.64	3.38	1.6	0.257	1.5	0.92
Kap_1875j.1.1	5.6E-6	100	0.110	0.44	0.18	0.67	0.76	1.1	0.01	187	90	41.6	7.5	0.50	0.18	1486	±20	1453	±21	1464	±22	1804	±8	+20	0.066	3.0	3.86	1.5	0.110	0.44	3.94	1.6	0.259	1.5	0.96
Kap_1875j.25.1	7.3E-5	58	0.094	0.99	0.65	0.49	0.52	1.4	0.13	63	109	14.1	9.2	1.79	0.32	1494	±23	1494	±25	1393	±33	1487	±22	-1	0.094	2.0	3.83	1.7	0.093	1.19	3.34	2.1	0.261	1.7	0.83
Kap_1875j.51.1	-2.7E-4	38	0.095	1.23	0.44	0.66	0.51	0.8	–	49	57	10.9	5.0	1.22	0.73	1496	±21	1486	±23	1425	±26	1596	±34	+7	0.094	2.1	3.83	1.6	0.099	1.85	3.55	2.4	0.261	1.6	0.65
Kap_1875j.45.1	-1.1E-4	50	0.094	1.03	0.67	0.54	0.71	1.4	–	39	67	8.8	6.0	1.77	0.42	1499	±21	1494	±23	1371	±29	1546	±24	+3	0.098	1.8	3.82	1.6	0.096	1.27	3.46	2.0	0.262	1.6	0.77
Kap_1875j.33.1	2.8E-5	58	0.094	0.62	0.17	1.24	0.60	3.8	0.05	132	58	29.8	5.2	0.45	0.73	1502	±23	1502	±25	1474	±24	1503	±13	+0	0.101	3.1	3.81	1.7	0.094	0.66	3.39	1.8	0.262	1.7	0.93
Kap_1875j.37.1	-4.2E-5	41	0.093	0.84	0.09	0.54	0.64	1.1	–	143	34	32.2	3.1	0.25	0.19	1503	±21	1502	±23	1489	±21	1509	±17	+0	0.099	4.5	3.81	1.5	0.094	0.88	3.40	1.8	0.263	1.5	0.87
Kap_1875j.2.1	1.8E-4	50	0.092	1.35	0.44	0.71	0.75	1.1	0.32	24	28	5.4	2.4	1.21	0.50	1507	±22	1516	±25	1444	±28	1419	±38	-7	0.098	2.2	3.80	1.7	0.090	1.98	3.26	2.6	0.263	1.7	0.65
Kap_1875j.7.1	3.1E-5	71	0.095	0.79	0.29	1.11	0.73	1.1	0.06	66	51	14.9	4.4	0.80	0.55	1510	±23	1509	±26	1469	±27	1513	±16	+0	0.096	2.6	3.79	1.7	0.094	0.85	3.43	1.9	0.264	1.7	0.90
Kap_1875j.40.1	-4.8E-4	35	0.094	1.57	0.30	0.96	0.38	1.2	--	39	32	8.8	2.8	0.84	0.45	1510	±22	1497	±24	1461	±25	1640	±51	+9	0.093	2.7	3.79	1.7	0.101	2.73	3.67	3.2	0.264	1.7	0.52
Kap_1875j.30.1	2.2E-5	71	0.094	0.65	0.12	1.86	0.77	1.4	0.04	83	27	18.8	2.3	0.33	1.38	1513	±21	1514	±23	1497	±22	1502	±13	-1	0.098	4.1	3.78	1.6	0.094	0.69	3.42	1.7	0.264	1.6	0.92
Kap_1875j.46.1	-1.6E-5	71	0.094	0.57	0.24	0.38	0.75	1.1	–	104	64	23.6	5.7	0.64	0.21	1515	±22	1515	±24	1477	±24	1516	±11	+0	0.100	2.2	3.77	1.6	0.094	0.59	3.45	1.7	0.265	1.6	0.94
Kap_1875j.22.1	1.2E-4	52	0.095	1.74	1.01	0.83	0.71	2.1	0.21	33	84	7.5	7.7	2.64	0.41	1526	±22	1529	±24	1288	±40	1499	±38	-2	0.103	1.9	3.74	1.6	0.094	1.99	3.44	2.5	0.267	1.6	0.62
Kap_1875j.50.1	–		0.093	1.18	0.64	0.56	0.53	0.5	0.00	46	77	10.7	6.9	1.74	0.38	1545	±21	1550	±24	1433	±30	1493	±22	-4	0.101	1.8	3.69	1.6	0.093	1.18	3.48	2.0	0.271	1.6	0.80
Kap_1875j.41.1	1.1E-4	33	0.111	0.65	0.13	1.06	0.53	0.3	0.20	113	40	27.4	3.5	0.37	0.64	1609	±23	1588	±25	1595	±24	1790	±15	+11	0.074	4.9	3.53	1.6	0.109	0.81	4.28	1.8	0.283	1.6	0.90
Kap_1875j.19.1	–		0.110	0.41	0.18	0.36	0.72	3.6	–	278	149	70.0	12.8	0.55	0.76	1655	±26	1638	±29	1640	±28	1793	±7	+9	0.083	3.5	3.42	1.8	0.110	0.41	4.42	1.8	0.293	1.8	0.97
Kap_1875j.12.1	-3.4E-5	58	0.109	0.63	0.35	0.39	0.69	1.9	–	81	76	20.9	7.4	0.97	0.25	1682	±22	1668	±24	1626	±25	1794	±12	+7	0.102	2.0	3.35	1.5	0.110	0.67	4.51	1.6	0.298	1.5	0.91
Kap_1875j.32.1	7.4E-5	58	0.108	0.94	0.20	0.73	0.75	2.0	0.13	40	21	10.5	2.1	0.54	0.38	1719	±23	1714	±26	1690	±25	1754	±20	+2	0.106	3.3	3.27	1.6	0.107	1.09	4.52	1.9	0.306	1.6	0.82
Kap_1875j.36.1	7.3E-5	35	0.110	0.56	0.24	1.34	0.61	1.7	0.13	160	106	42.3	10.0	0.68	0.72	1728	±26	1720	±29	1699	±29	1789	±12	+4	0.101	3.2	3.25	1.7	0.109	0.65	4.64	1.8	0.307	1.7	0.93
Kap_1875j.27.1	1.5E-4	35	0.110	0.80	0.34	0.51	0.83	2.2	0.27	52	47	13.7	4.7	0.93	0.34	1729	±23	1724	±26	1673	±27	1765	±19	+2	0.109	2.2	3.25	1.5	0.108	1.06	4.58	1.9	0.308	1.5	0.82
Kap_1875j.15.1	-1.6E-4	71	0.110	1.66	1.51	1.14	0.59	2.4	–	17	71	4.6	7.1	4.22	1.32	1742	±37	1730	±42	1271	±121	1831	±38	+6	0.110	3.1	3.22	2.4	0.112	2.10	4.79	3.2	0.310	2.4	0.76
Kap_1875j.21.1	4.4E-5	45	0.110	0.55	0.15	0.48	0.50	1.2	0.08	195	83	52.7	8.1	0.44	0.68	1760	±25	1756	±29	1741	±27	1793	±11	+2	0.104	3.9	3.18	1.7	0.110	0.61	4.74	1.8	0.314	1.7	0.94
Kap_1875j.24.1	3.1E-5	71	0.110	0.74	0.35	0.47	0.68	1.1	0.06	78	73	20.9	7.3	0.97	0.29	1761	±23	1758	±26	1705	±27	1784	±15	+1	0.111	2.2	3.18	1.5	0.109	0.80	4.72	1.7	0.314	1.5	0.88
Kap_1875j.39.1	–		0.107	0.97	0.48	0.54	0.62	1.0	–	46	62	12.3	6.0	1.41	0.37	1763	±29	1765	±33	1697	±36	1749	±18	-1	0.108	2.4	3.18	1.9	0.107	0.97	4.64	2.1	0.315	1.9	0.89
Kap_1875j.16.1	-2.1E-5	58	0.110	0.50	0.17	0.87	0.78	1.3	–	136	61	37.0	6.3	0.46	0.64	1772	±25	1768	±28	1745	±26	1803	±9	+2	0.111	3.6	3.16	1.6	0.110	0.52	4.81	1.7	0.316	1.6	0.95
Kap_1875j.38.1	1.3E-4	35	0.109	0.75	0.33	2.59	0.80	0.8	0.23	54	48	14.7	4.8	0.92	2.63	1778	±23	1781	±27	1729	±29	1757	±17	-1	0.114	4.3	3.15	1.5	0.107	0.95	4.71	1.8	0.318	1.5	0.85
Kap_1875j.29.1	-5.4E-5	58	0.109	0.79	0.13	0.74	0.90	1.4	–	47	16	13.0	1.7	0.35	0.35	1799	±28	1799	±32	1774	±29	1796	±16	-0	0.123	5.0	3.11	1.8	0.110	0.87	4.87	2.0	0.322	1.8	0.90
Kap_1875j.44.1	-1.2E-4	35	0.111	0.73	0.24	2.14	0.86	1.3	–	51	33	14.2	3.6	0.66	2.03	1801	±28	1795	±32	1755	±32	1839	±16	+2	0.117	4.3	3.10	1.8	0.112	0.88	5.00	2.0	0.322	1.8	0.90
Kap_1875j.3.1	-7.2E-5	45	0.110	0.71	0.21	0.54	0.77	1.8	–	74	42	21.0	4.6	0.59	0.29	1833	±24	1836	±28	1795	±26	1815	±15	-1	0.123	3.0	3.04	1.5	0.111	0.80	5.03	1.7	0.329	1.5	0.88
Kap_1875j.20.1	9.7E-6	100	0.110	0.58	0.20	0.89	0.89	2.0	0.02	91	48	25.8	5.2	0.54	0.47	1836	±30	1842	±35	1801	±33	1796	±11	-3	0.125	3.8	3.04	1.9	0.110	0.59	4.99	2.0	0.329	1.9	0.95
Kap_1875j.4.1	-4.4E-5	58	0.110	0.71	0.13	0.66	0.96	0.4	–	49	17	14.0	1.9	0.37	1.06	1862	±32	1869	±37	1839	±33	1817	±14	-3	0.131	5.5	2.99	2.0	0.111	0.77	5.13	2.1	0.335	2.0	0.93
Kap_1875j.34.1	-9.2E-5	41	0.113	0.72	0.16	1.12	0.85	1.0	–	52	23	15.1	2.4	0.45	0.96	1871	±27	1873	±32	1845	±29	1863	±15	-1	0.122	4.5	2.97	1.7	0.114	0.84	5.29	1.9	0.337	1.7	0.90
Kap_1875j.31.2	4.0E-5	100	0.078	1.39	0.140	1.08	0.49	0.6	0.073	69	25	10.8	1.5	0.38	0.39	1083	19	1080	19	1070	20	1125	32	+4	0.065	3.5	5.47	1.9	0.077	1.59	1.9	2.4	0.183	1.9	0.76
Kap_1875j.77.1	1.1E-4	38	0.080	0.85	0.140	0.67	0.48	2.4	0.196	133	48	21.9	3.0	0.37	0.26	1128	21	1125	22	1115	22	1167	23	+4	0.068	3.1	5.23	2.0	0.079	1.14	2.1	2.3	0.191	2.0	0.87
Kap_1875j.10.2	-6.1E-5	71	0.079	1.23	0.353	0.65	0.43	0.5	-0.110	97	90	16.0	5.7	0.95	0.32	1129	19	1126	20	1090	22	1191	28	+6	0.070	2.2	5.22	1.8	0.080	1.44	2.1	2.3	0.191	1.8	0.79
Kap_1875j.54.1	4.3E-4	27	0.080	1.20	0.145	2.23	0.55	0.5	0.770	60	22	10.7	1.4	0.37	1.41	1203	20	1212	22	1194	22	1048	52	-16	0.080	4.1	4.87	1.9	0.074	2.56	2.1	3.2	0.205	1.9	0.59
Kap_1875j.42.2	-2.4E-4	33	0.078	1.13	0.112	0.97	0.51	1.0	-0.436	96	28	17.1	2.1	0.30	0.32	1220	25	1219	27	1203	26	1228	35	+1	0.083	4.1	4.80	2.3	0.081	1.76	2.3	2.9	0.208	2.3	0.79
Kap_1875j.58.1	9.3E-6	100	0.093	0.96	0.244	0.41	0.47	1.9	0.017	225	149	44.7	11.0	0.68	0.35	1342	22	1330	23	1316	24	1490	18	+11	0.076	2.5	4.32	1.8	0.093	0.97	3.0	2.1	0.231	1.8	0.88
Kap_1875j.25.2	2.4E-4	38	0.093	1.16	0.611	1.84	0.50	1.9	0.428	67	111	13.6	8.3	1.71	1.48	1363	28	1358	30	1288	40	1428	35	+5	0.082	3.4	4.25	2.3	0.090	1.85	2.9	2.9	0.235	2.3	0.78
Kap_1875j.66.1	-1.3E-4	58	0.095	2.13	0.711	0.61	0.78	1.1	-0.240	38	68	8.2	5.9	1.85	0.50	1439	25	1427	27	1300	36	1570	44	+9	0.094	2.3	4.00	1.9	0.097	2.35	3.3	3.1	0.250	1.9	0.64
Kap_1875j.74.1	7.8E-5	41	0.094	0.72	0.551	0.61	0.51	1.9	0.141	151	220	33.5	18.6	1.50	0.38	1477	25	1476	27	1393	33	1494	16	+1	0.094	2.2	3.88	1.9	0.093	0.87	3.3	2.1	0.258	1.9	0.91
Kap_1875j.63.1	-3.6E-5	71	0.093	0.85	0.253	1.26	0.56	0.4	-0.065	100	66	22.4	5.7	0.68	1.12	1489	26	1489	29	1452	29	1490	18	+0	0.097	3.2	3.85	2.0	0.093	0.93	3.3	2.2	0.260	2.0	0.91
Kap_1875j.64.1	-8.8E-5	50	0.095	0.93	0.304	0.58	0.69	2.1	-0.159	70	54	15.7	4.9	0.79	1.47	1497	24	1493	27	1445	28	1543	21	+3	0.099	2.8	3.83	1.8	0.096	1.12	3.5	2.1	0.261	1.8	0.85
Kap_1875j.73.1	-2.4E-5	71	0.094	0.69	0.273	0.88	0.67	2.2	-0.043	114	78	25.6	7.1	0.71	0.25	1498	26	1496	28	1452	29	1521	14	+2	0.100	2.6	3.82	1.9	0.095	0.73	3.4	2.0	0.262	1.9	0.93
Kap_1875j.55.1	–		0.094	1.00	0.419	1.82	0.69	1.7	0.000	57	58	13.0	5.5	1.05	1.95	1513	32	1514	35	1430	39	1505	19	-1	0.106	3.8	3.78	2.3	0.094	1.00	3.4	2.5	0.264	2.3	0.92
Kap_1875j.70.1	-2.2E-5	71	0.094	0.66	0.337	0.89	0.66	1.4	-0.039	127	110	28.8	9.8	0.90	0.23	1516	26	1516	28	1462	30	1520	13	+0	0.099	2.5	3.77	1.9	0.095	0.69	3.5	2.0	0.265	1.9	0.94
Kap_1875j.59.1	5.0E-5	58	0.094	0.82	0.046	1.16	0.65	1.2	0.091	79	14	18.1	0.8	0.18	0.99	1526	24	1529	27	1532	25	1501	18	-2	0.071	9.5	3.74	1.8	0.094	0.93	3.4	2.0	0.267	1.8	0.89
Kap_1875j.79.1	-4.2E-5	58	0.094	0.75	0.444	0.40	0.65	1.8	-0.076	110	126	25.4	11.4	1.18	0.26	1531	25	1533	27	1455	30	1521	16	-1	0.102	2.1	3.73	1.8	0.095	0.83	3.5	2.0	0.268	1.8	0.91
Kap_1875j.57.1	-8.2E-5	58	0.096	1.03	0.212	0.74	0.63	1.3	-0.147	73	41	16.9	3.7	0.57	1.29	1544	25	1543	28	1512	28	1561	23	+1	0.100	3.3	3.69	1.8	0.097	1.22	3.6	2.2	0.271	1.8	0.83
Kap_1875j.60.1	-1.3E-4	45	0.094	1.03	0.312	0.62	0.39	1.9	-0.233	127	108	29.7	9.5	0.87	0.50	1549	25	1549	28	1504	29	1549	25	+0	0.098	2.5	3.68	1.8	0.096	1.31	3.6	2.2	0.272	1.8	0.81
Kap_1875j.67.1	-4.0E-5	41	0.111	0.48	0.232	0.91	0.63	2.0	-0.072	264	217	61.9	14.5	0.85	0.30	1555	24	1525	26	1567	27	1823	9	+17	0.060	2.9	3.66	1.8	0.111	0.52	4.2	1.8	0.273	1.8	0.96
Kap_1875j.69.1	1.4E-5	58	0.108	0.41	0.340	0.54	0.86	1.8	0.025	263	234	70.3	24.1	0.92	0.17	1745	29	1743	33	1685	34	1764	8	+1	0.114	2.6	3.22	1.9	0.108	0.42	4.6	2.0	0.311	1.9	0.98
Kap_1875j.78.1	-3.7E-5	32	0.110	0.56	0.145	0.32	0.87	2.1	-0.066	270	108	72.2	10.7	0.41	0.37	1749	27	1741	30	1728	28	1803	10	+3	0.103	4.3	3.21	1.7	0.110	0.58	4.7	1.8	0.312	1.7	0.95
Kap_1875j.65.1	1.5E-5	100	0.110	0.72	0.246	1.58	0.74	1.8	0.027	96	62	25.6	6.4	0.67	0.33	1749	32	1744	36	1707	36	1791	14	+3	0.112	3.8	3.21	2.1	0.109	0.75	4.7	2.2	0.312	2.1	0.94
Kap_1875j.80.1	2.6E-5	49	0.110	1.22	0.242	1.24	0.85	2.3	0.047	172	109	47.1	11.5	0.66	0.62	1789	43	1787	49	1747	47	1799	22	+1	0.116	5.0	3.13	2.7	0.110	1.23	4.8	3.0	0.320	2.7	0.91
Kap_1875j.71.1	4.0E-5	41	0.111	0.47	0.273	0.57	0.74	1.2	0.072	233	172	64.1	17.6	0.76	0.41	1790	30	1787	34	1747	33	1812	9	+1	0.112	3.0	3.12	1.9	0.111	0.52	4.9	2.0	0.320	1.9	0.96
Kap_1875j.68.1	7.2E-5	38	0.111	0.59	0.188	0.48	0.81	2.1	0.129	122	60	33.7	6.3	0.51	0.55	1798	28	1797	32	1767	30	1805	12	+0	0.117	3.7	3.11	1.8	0.110	0.68	4.9	1.9	0.322	1.8	0.93
Kap_1875j.76.1	6.6E-5	58	0.109	0.88	0.439	0.51	0.80	1.4	0.120	63	72	17.5	7.7	1.18	0.37	1806	29	1810	34	1720	36	1773	18	-2	0.122	2.4	3.09	1.8	0.108	1.01	4.8	2.1	0.323	1.8	0.88
Kap_1875j.52.1	-4.2E-5	71	0.110	0.85	0.205	0.66	0.86	1.7	-0.076	59	31	16.3	3.4	0.54	0.37	1806	29	1807	33	1766	32	1801	17	-0	0.124	3.7	3.09	1.8	0.110	0.93	4.9	2.1	0.323	1.8	0.89
Kap_1875j.62.1	-3.6E-5	45	0.110	0.50	0.225	1.06	0.89	1.2	-0.066	168	99	47.2	10.8	0.61	0.43	1820	37	1822	43	1778	41	1809	10	-1	0.123	4.2	3.07	2.3	0.111	0.54	5.0	2.4	0.326	2.3	0.97
Kap_1875j.61.1	-2.3E-5	50	0.114	0.44	0.065	3.17	0.76	2.9	-0.042	222	38	62.5	4.1	0.18	2.15	1828	29	1823	34	1816	30	1862	8	+2	0.110	11.1	3.05	1.8	0.114	0.46	5.1	1.9	0.328	1.8	0.97
Kap_1875j.53.1	-3.4E-5	38	0.112	0.41	0.110	0.41	0.84	1.5	-0.062	217	63	61.9	7.0	0.30	0.18	1844	28	1844	33	1823	29	1842	8	-0	0.124	5.6	3.02	1.8	0.113	0.44	5.1	1.8	0.331	1.8	0.97
Kap_1875j.72.1	1.5E-5	100	0.112	0.72	0.187	0.58	0.72	1.9	0.027	110	56	31.4	5.9	0.53	0.29	1846	32	1848	37	1818	35	1833	13	-1	0.119	4.3	3.02	2.0	0.112	0.74	5.1	2.1	0.332	2.0	0.94
Kap_1875j.56.1	-2.3E-5	41	0.113	0.36	0.099	1.74	0.88	1.6	-0.041	267	70	77.3	7.8	0.27	1.56	1872	28	1875	33	1855	30	1854	7	-1	0.130	6.6	2.97	1.8	0.113	0.37	5.3	1.8	0.337	1.8	0.98
Kap_1875j.75.1	9.7E-6	100	0.121	0.55	0.162	0.49	0.89	0.7	0.017	106	46	30.9	5.0	0.45	0.25	1880	29	1865	33	1854	31	1972	10	+5	0.107	4.8	2.95	1.8	0.121	0.56	5.7	1.9	0.339	1.8	0.95

Errors are 1-sigma; Pb_c and Pb^* indicate the common and radiogenic portions. respectively.

Error in Standard calibration was 0.34% (not included in above errors but required when comparing data from different mounts).

(1) Common Pb corrected using measured 204Pb.

(2) Common Pb corrected by assuming 206Pb/238U-207Pb/235U age-concordance

(3) Common Pb corrected by assuming 206Pb/238U-208Pb/232Th age-concordance